Electromagnetic precursor flaring in binary neutron star mergers

LRAC AST20008

Elias Roland Most

Bart Ripperda, Alexander Philippov (PI)

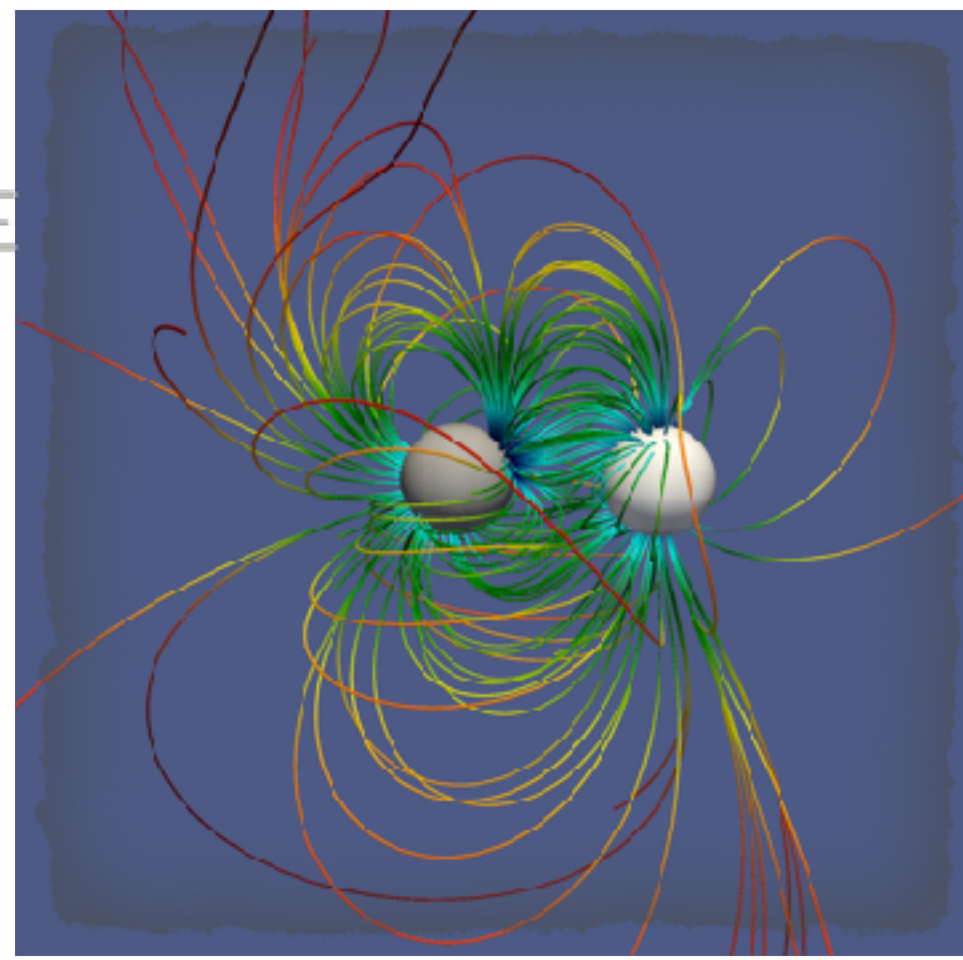

The final fate of a neutron star binary

Gravitational waves

sGRB

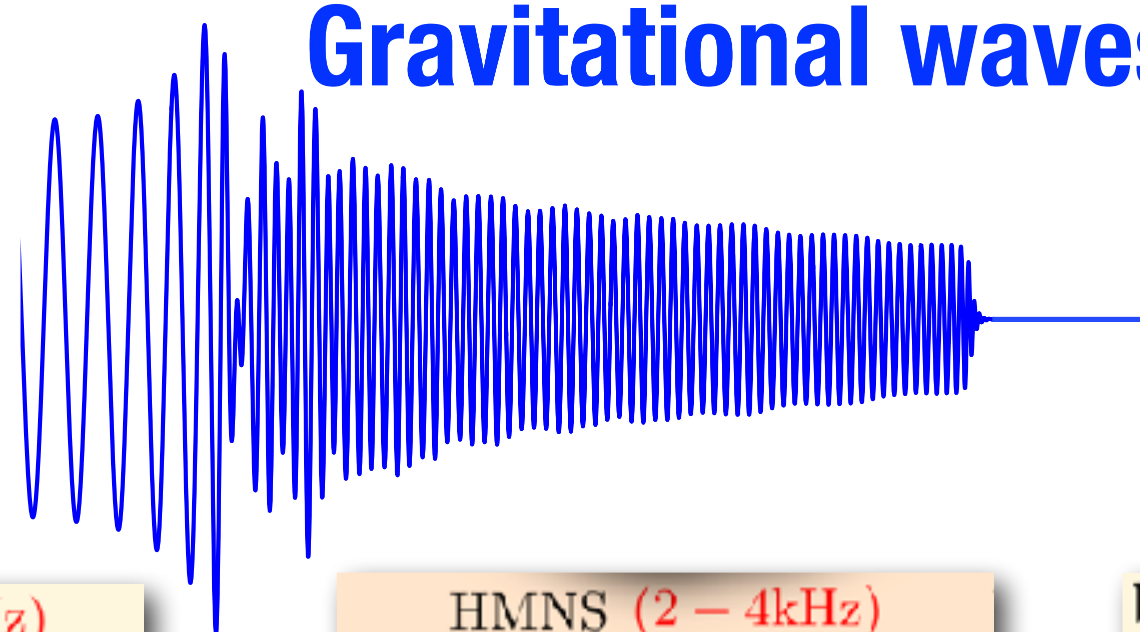

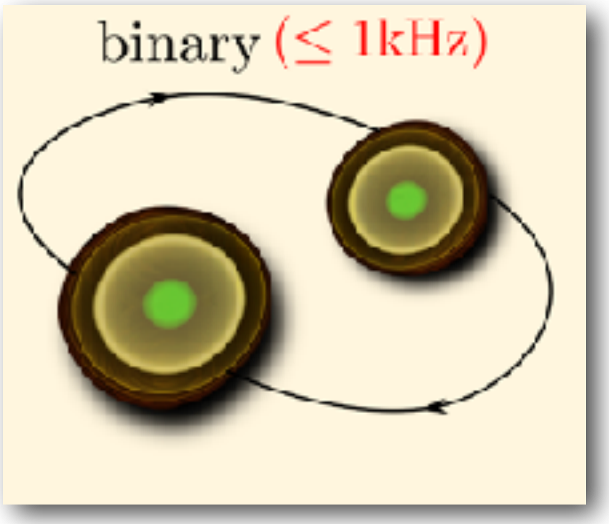

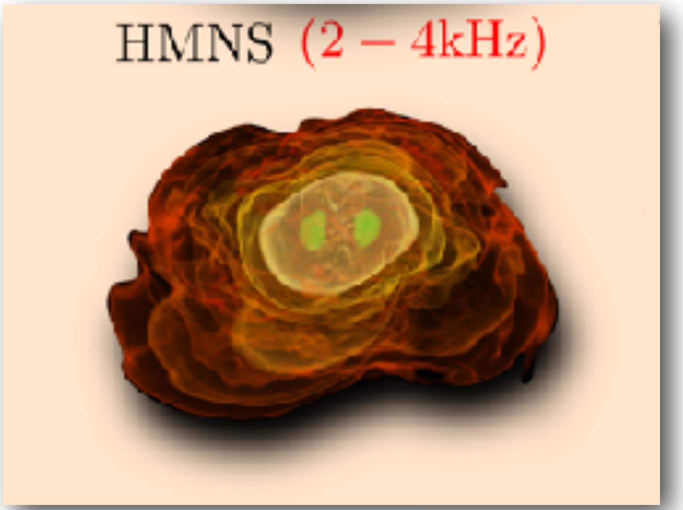

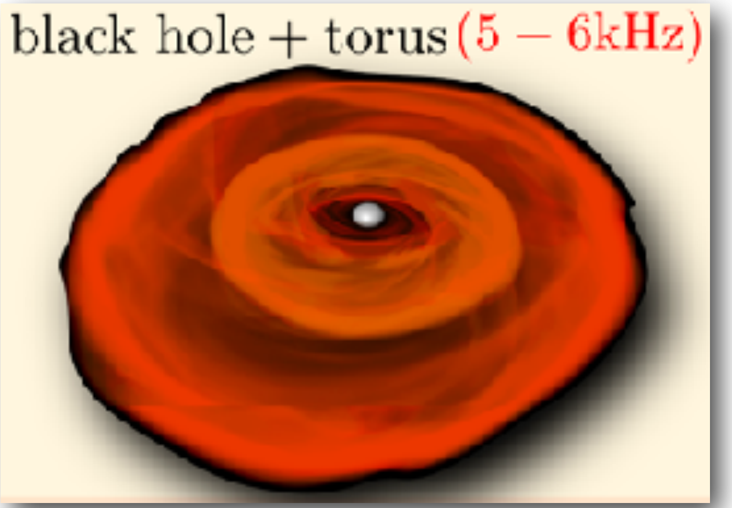

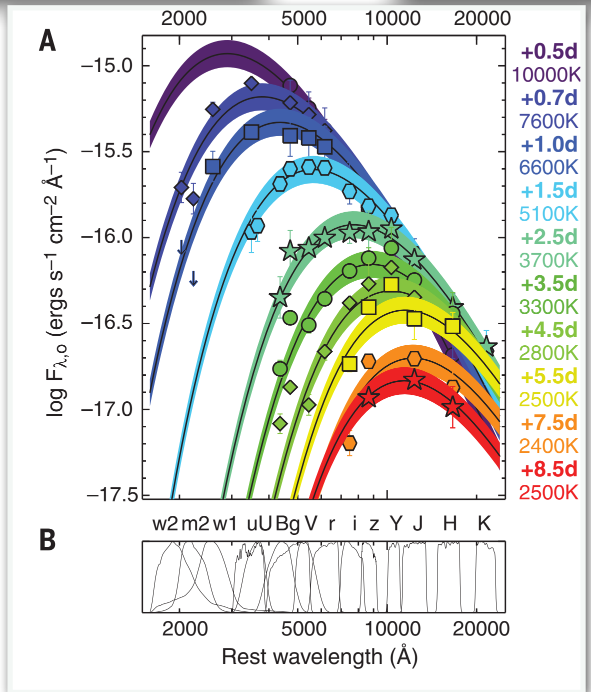

Kilonova

Afterglow

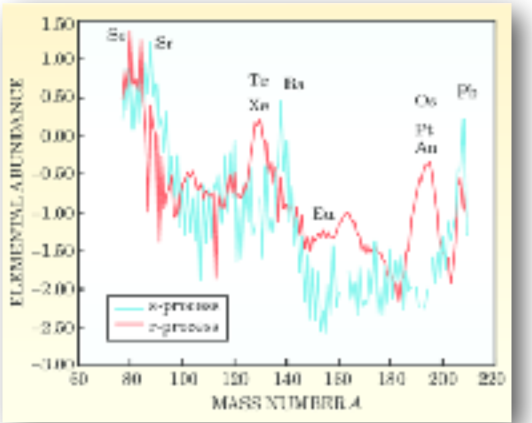

The final fate of a neutron star binary

Gravitational waves

sGRB

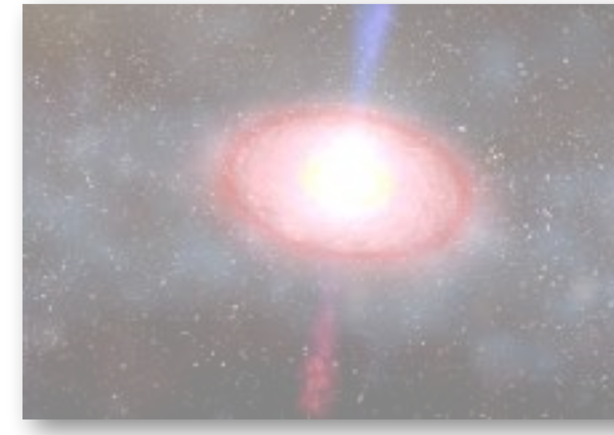

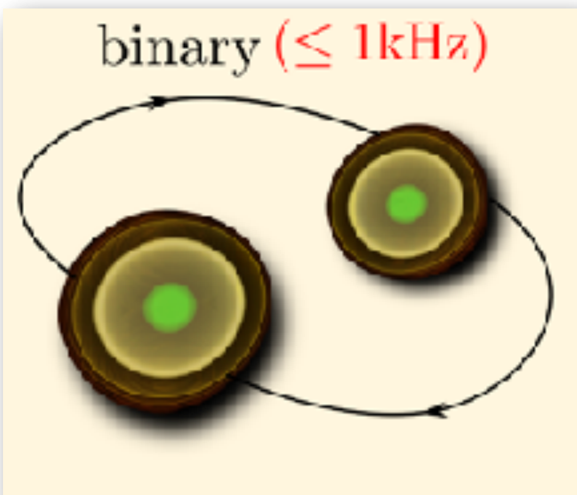

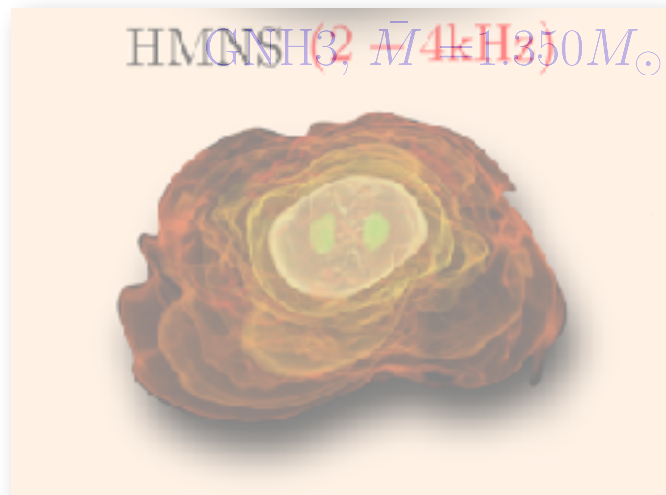

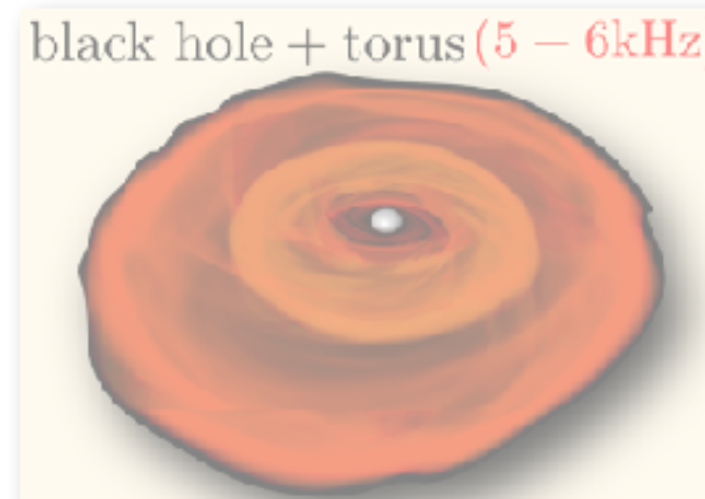

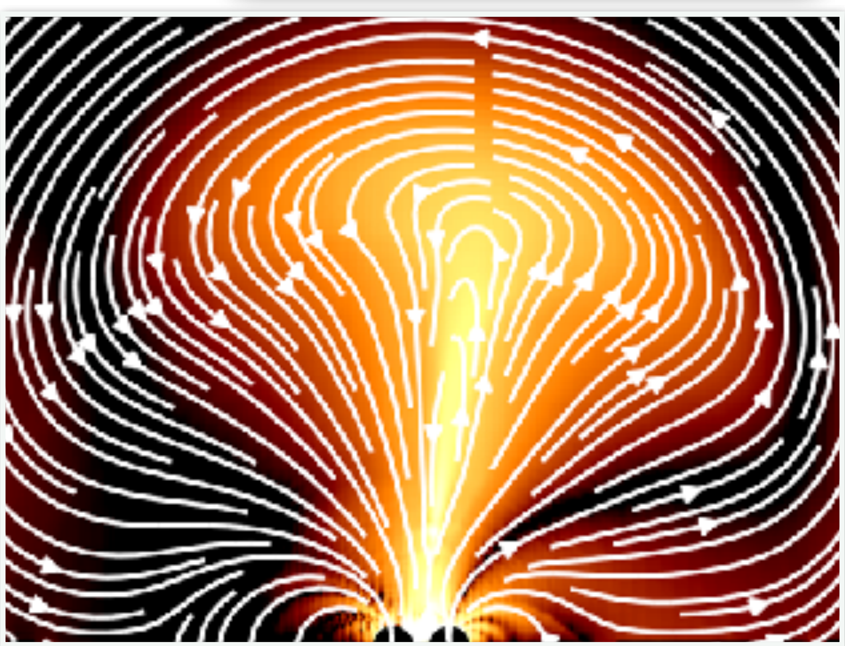

Precursor Emission ???

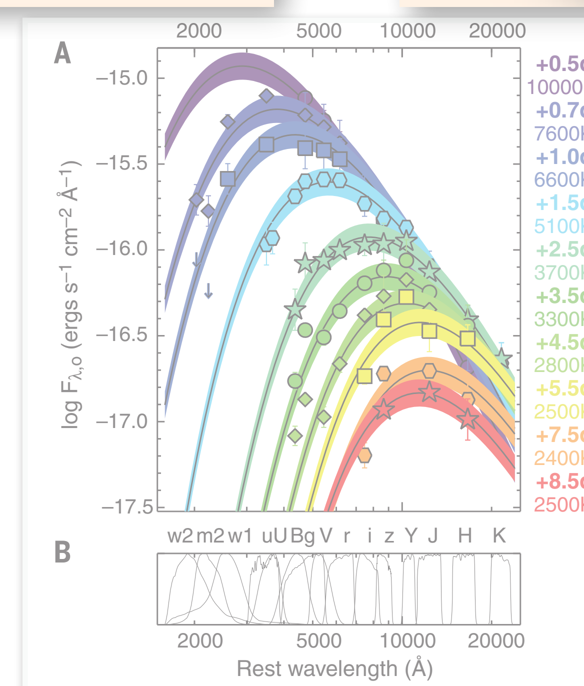

Kilonova

Afterglow

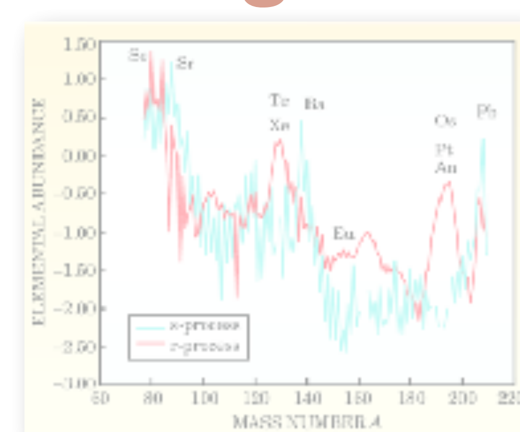

Electromagnetic precursors

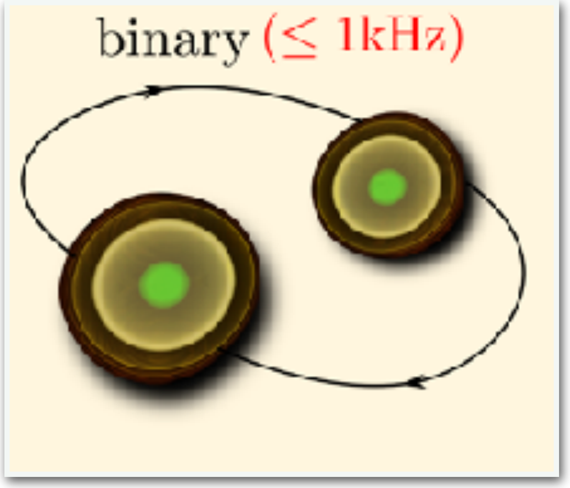

- Magnetospheric interaction can release of significant amounts of EM energy
- EM precursors can constrain binary parameters (e.g. spin)

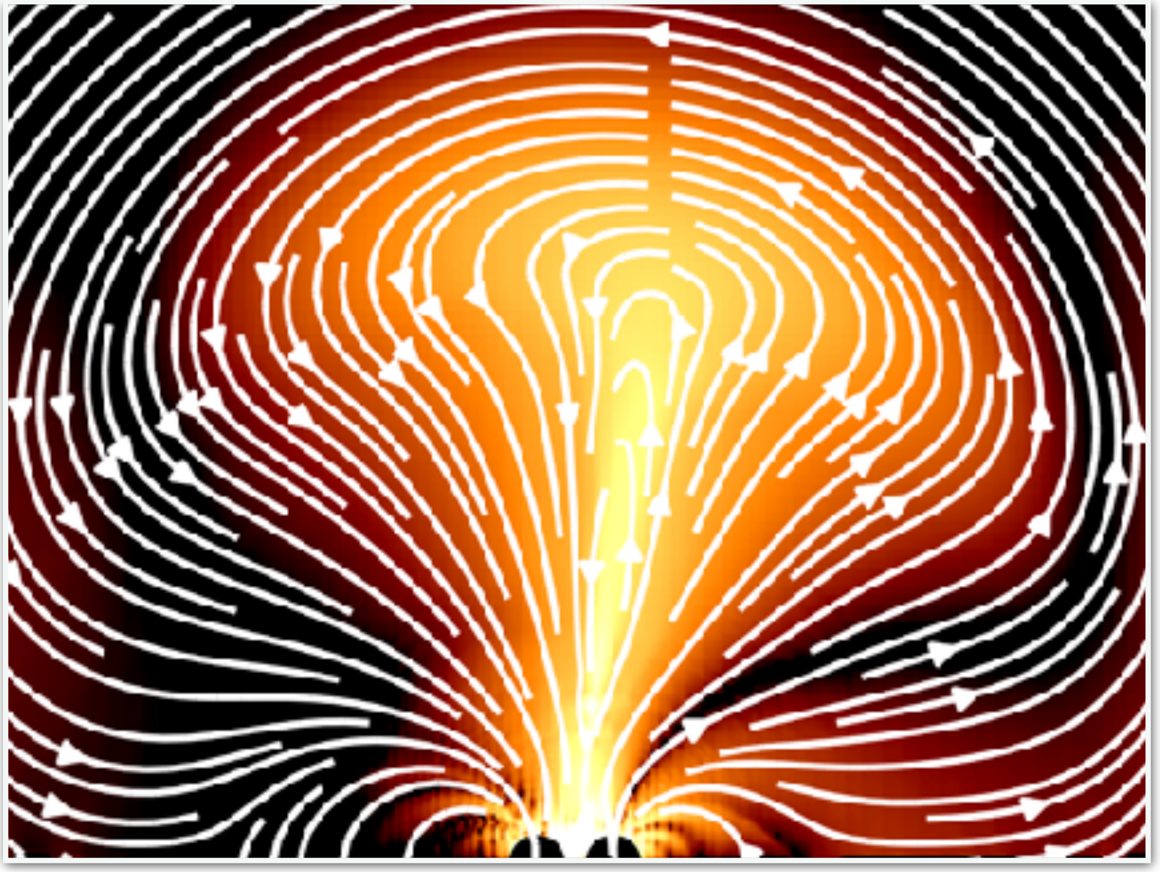

ERM & Philippov (ApJL 2020)

$$\mathscr{L}_{\rm diss} = 7.4 \times 10^{42}\, \zeta_\phi \left(\frac{B_*}{10^{12}\,{\rm G}}\right)^2 \left(\frac{a}{30\,{\rm km}}\right)^{-13/2} {\rm erg\ s^{-1}}$$

Lai (2012)

Twisting of field lines can enhance emission ($\zeta_\phi \gg 1$)

Spinning neutron stars

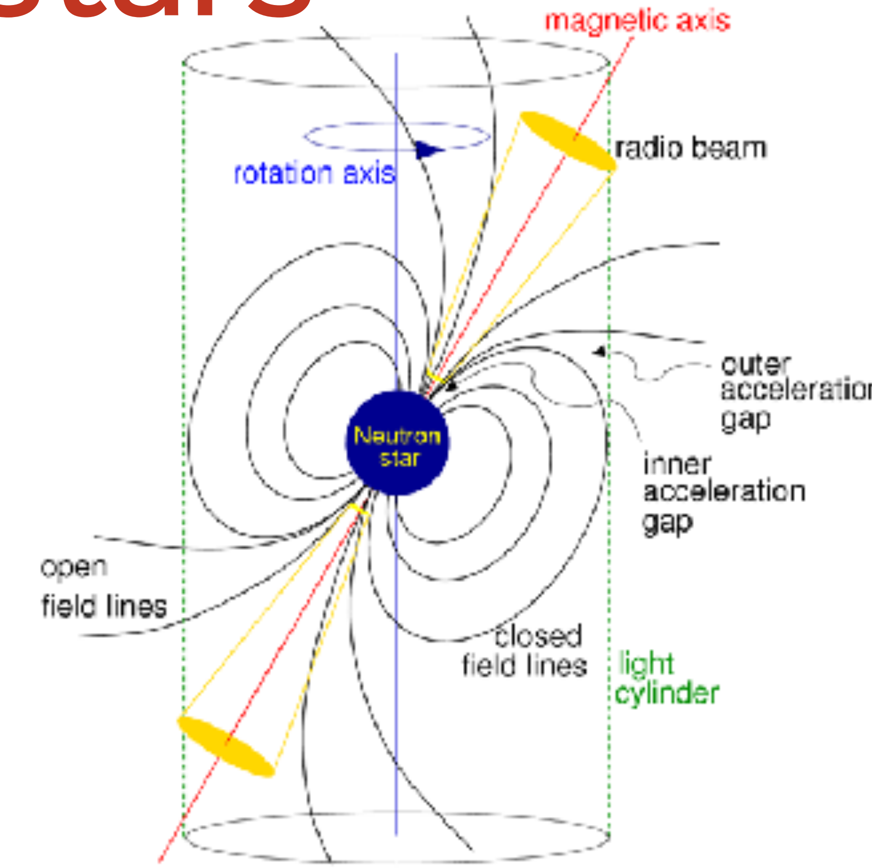

- Rotating neutron stars are observed as radio pulsars.
- Their rotation rate can be accurately measured from the radio signal.
- Pulsars are thought to be born slowly rotating, spin-up requires mass accretion from a companion
- Fastest spinning pulsar PSR J1748−2446ad rotates at $P \approx 1.4\,\mathrm{ms}$

Hessels+ (2006)

Lorimer & Kramer (2004)

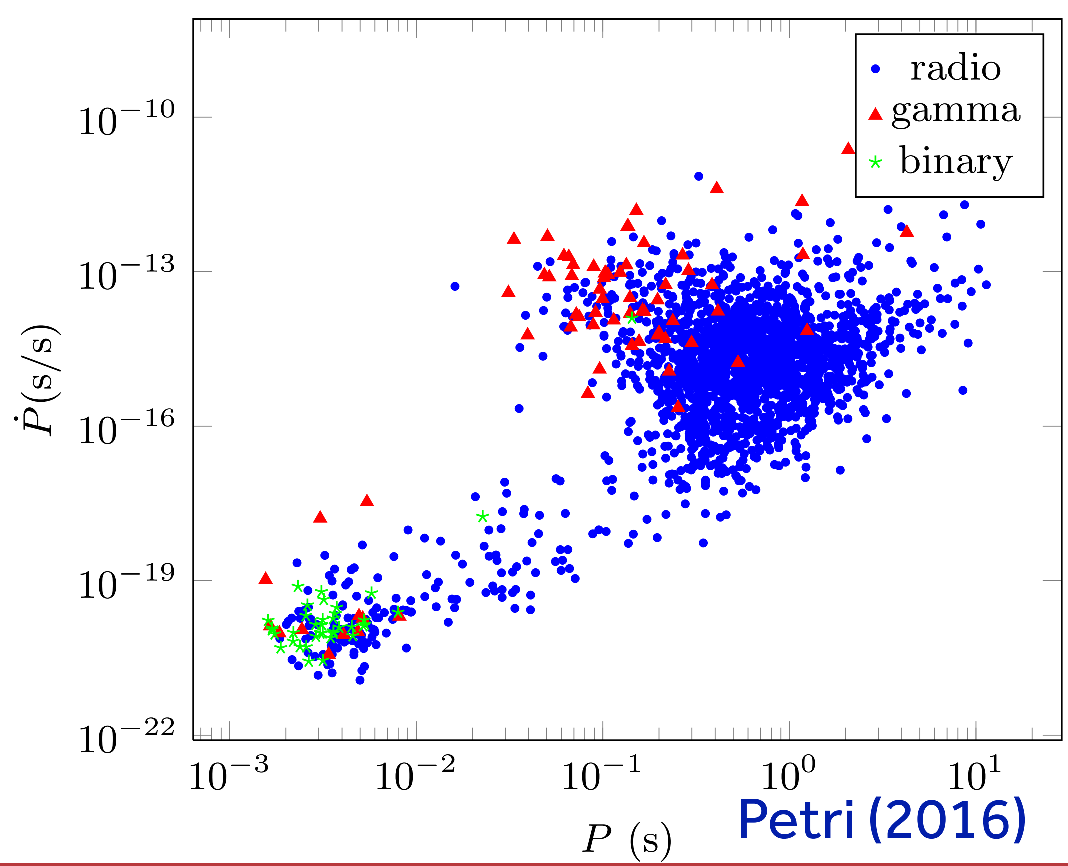

Petri (2016)

Pulsar magnetospheres

- Pulsars are equipped force-free magnetospheres consisting of a highly conducting $e^- - e^+$ pair plasma Goldreich&Julian (1969)

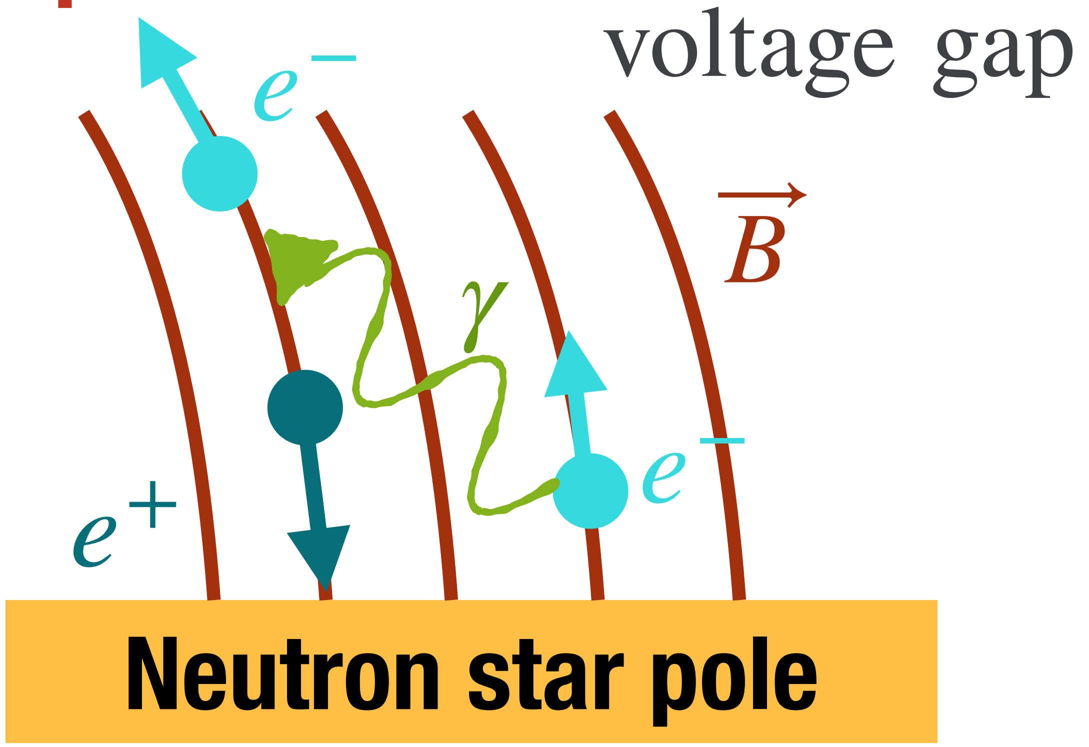

Pulsar magnetospheres

- Pulsars are equipped force-free magnetospheres consisting of a highly conducting $e^- - e^+$ pair plasma Goldreich&Julian (1969)
- Field lines beyond the light cylinder open up

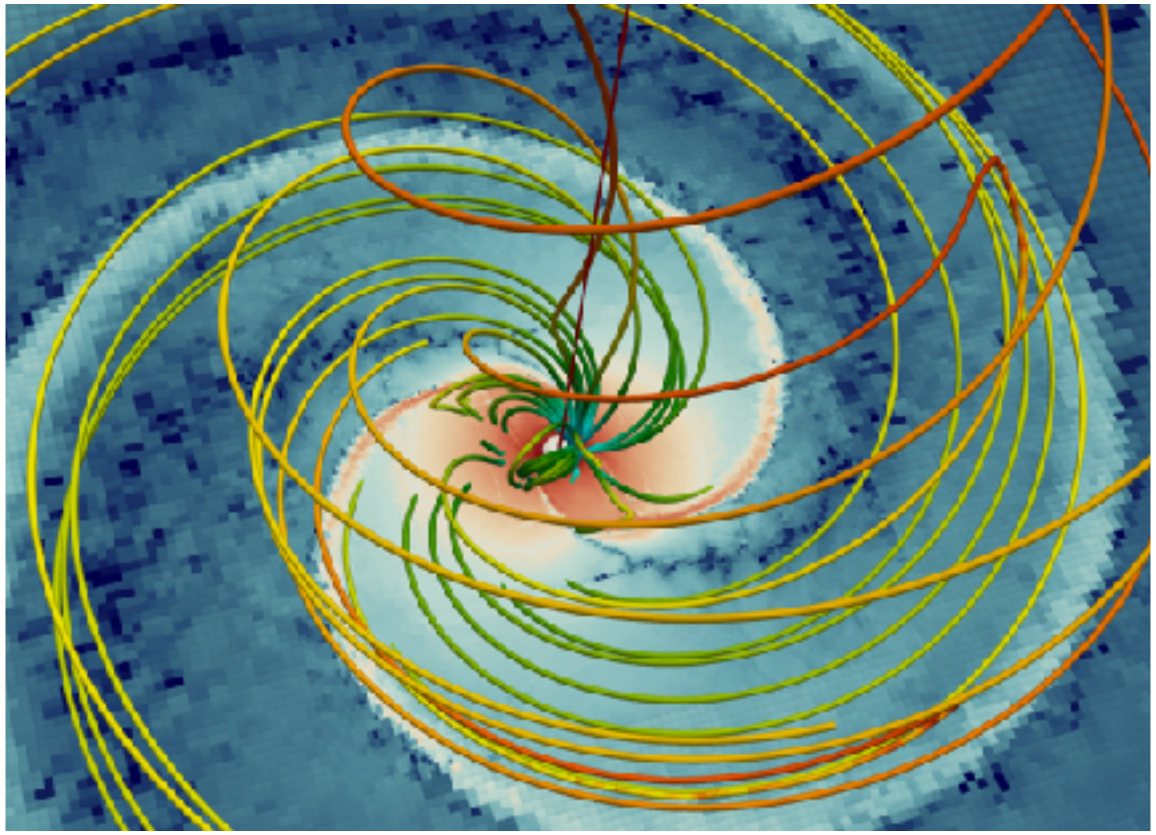

Pulsar magnetospheres

- Pulsars are equipped force-free magnetospheres consisting of a highly conducting $e^{-} - e^{+}$ pair plasma Goldreich&Julian (1969)
- Field lines beyond the light cylinder open up
- Strong current sheets are present that might be responsible for some of the coherent radio emission

Philippov+(2019)

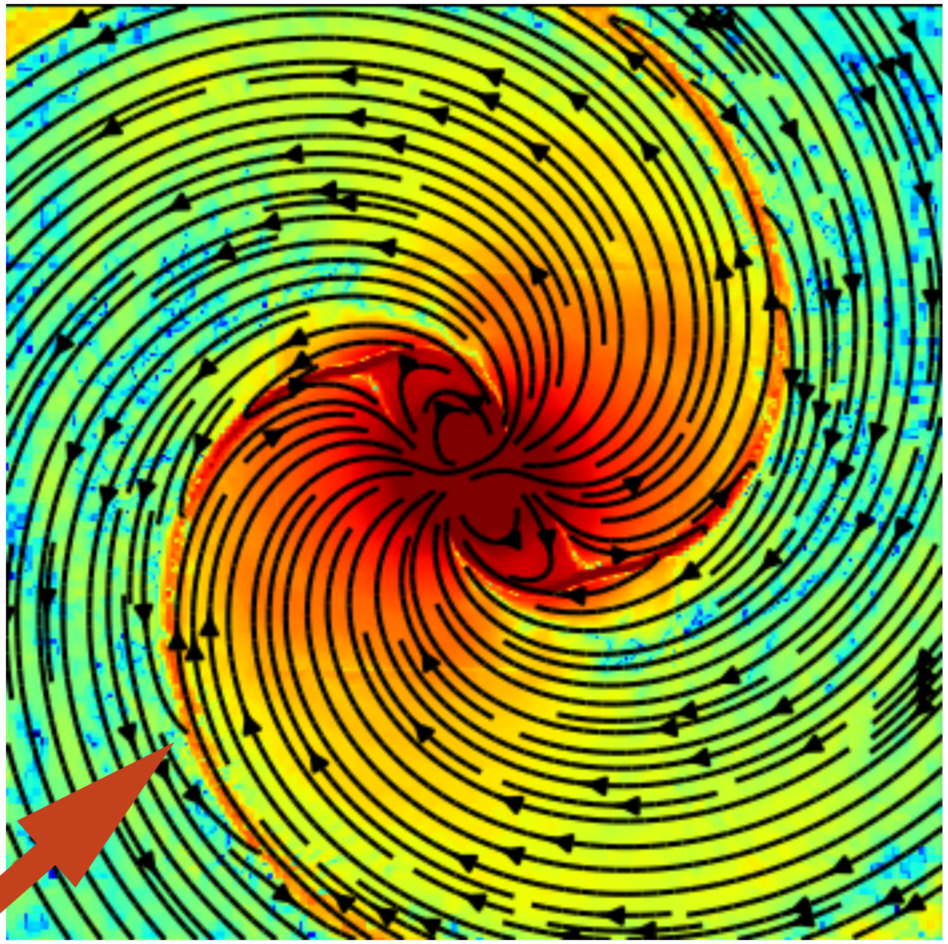

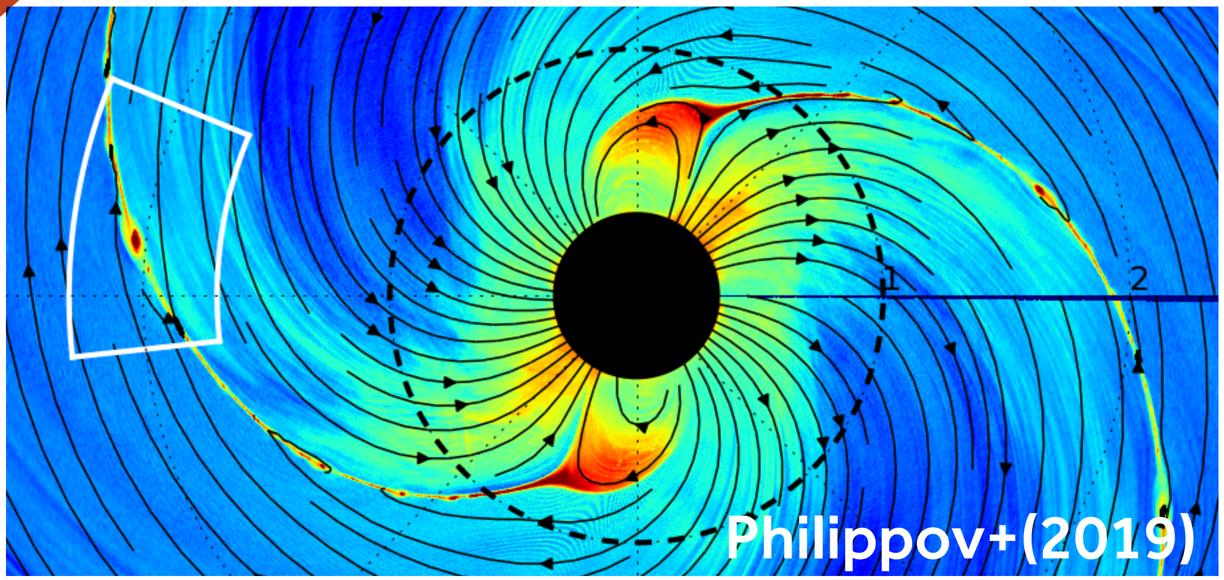

GReX code

ERM+ (in prep)

$$\nabla_\mu \left(T^{\mu\nu}_{\rm hydro} + T^{\mu\nu}_{\rm EM} \right) = 0 \qquad G_{\mu\nu} = \frac{8\pi G}{c^4} \left(T^{\mu\nu}_{\rm hydro} + T^{\mu\nu}_{\rm EM} \right)$$

- GRMHD with dynamical spacetime, both fourth order accurate $\hat{f}^i = f^i + \frac{1}{24}\Delta^2 f^i$
- Solves GRMHD in local frame with optional HLLD Riemann solver
- Dynamical space-time evolution using Z4c
- Full dynamical AMR capability through AMReX framework
- Recently extended to fully resistive GRMHD with force-free coupling

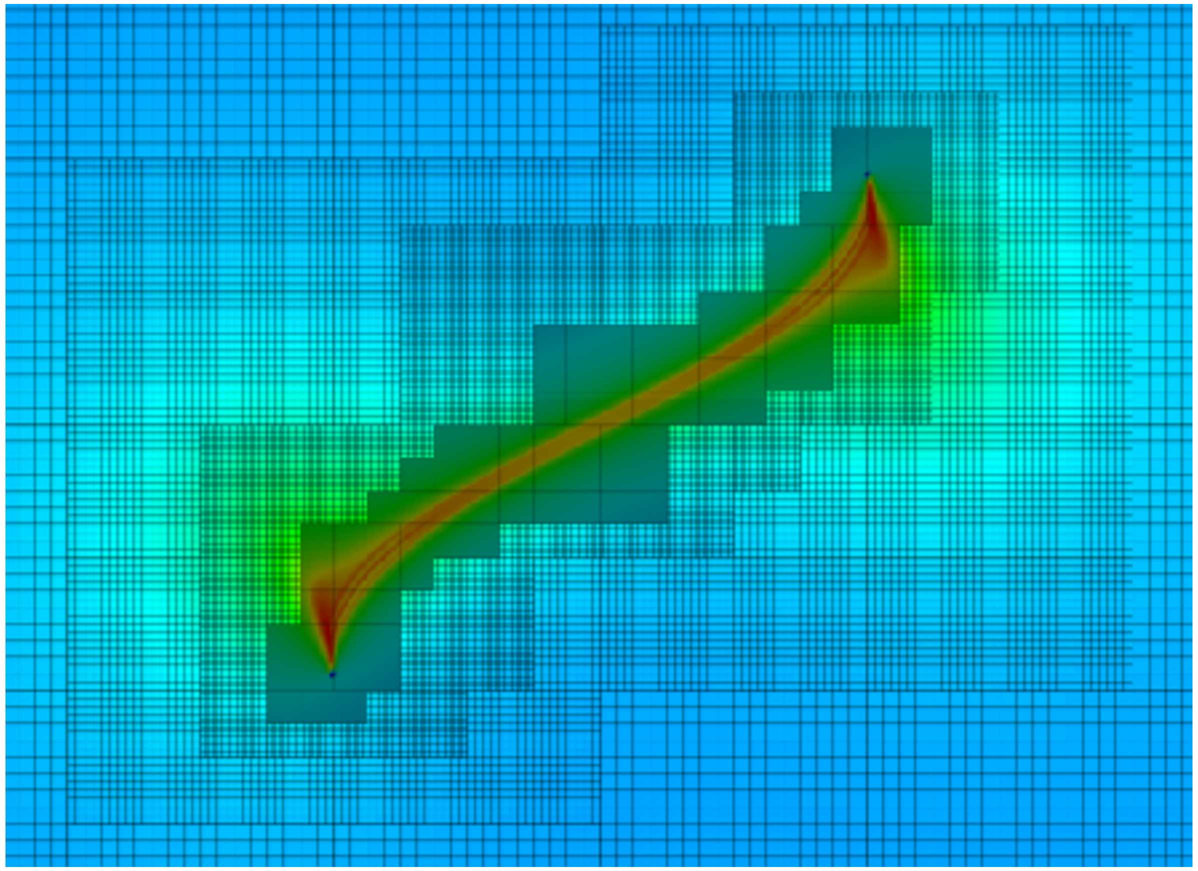

Binary black holes in ambient gas

Adaptive mesh refinement in simulations of binary neutron star mergers

- At the time of merger a shear layer forms at the contact interface of the two stars
- Additional perpendicular compression due to gravity between the two stars

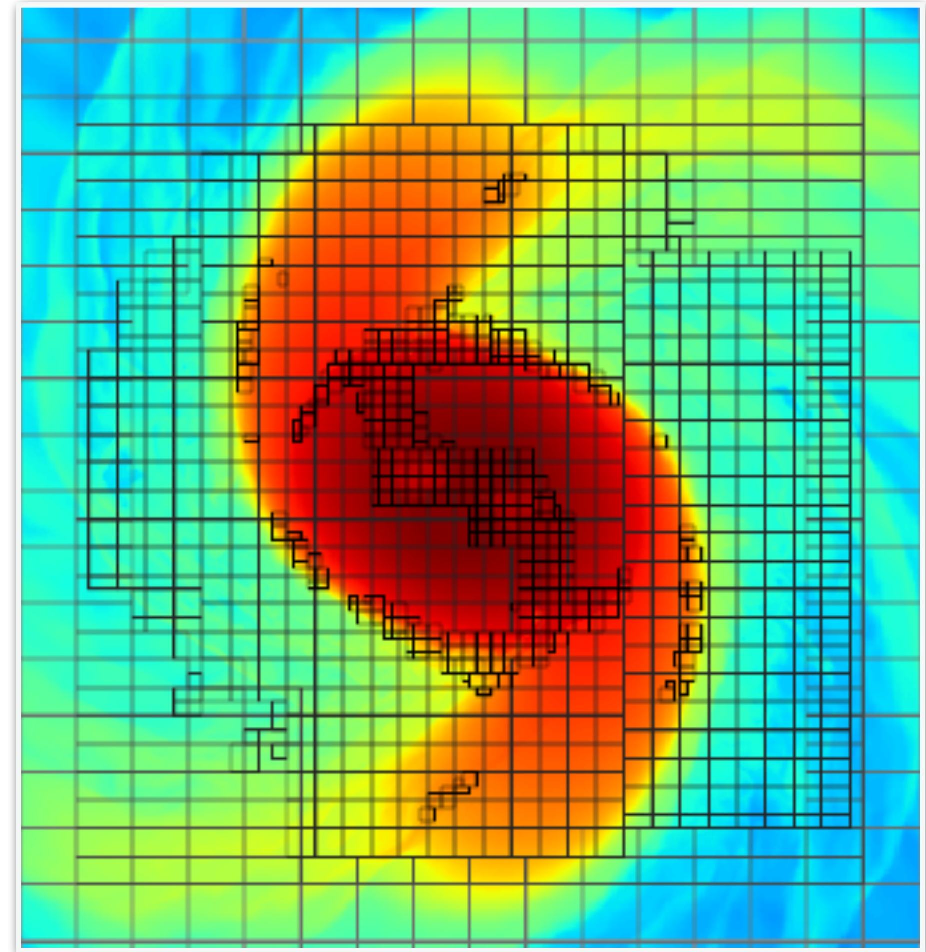

ERM+ (in prep)

ERM+ (in prep)

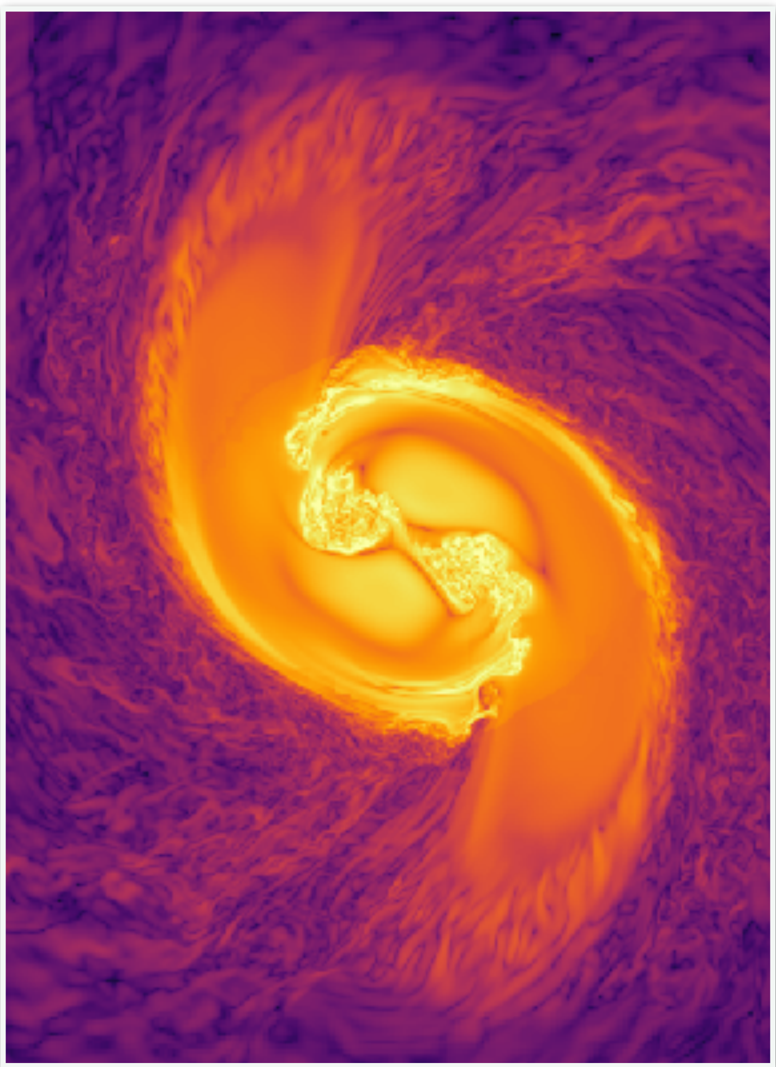

35m resolution
on 12,000 cores
computed with GReX

- Kelvin-Helmholtz instability can amplify the magnetic field strength by several orders of magnitude Kiuchi+(2015,2018)

Exploratory dynamo studies with V. Skoutnev & A. Bhattacharjee (PPPL)

Under the hood

- All computationally heavy routines have been written using modern C++17 expression templates and zero-overhead parallel data types

- Allows to write easily maintainable code that will be converted to intrinsics at compile time(even with many branches)

$$R_{ij}^{W} = \frac{1}{W}\tilde{D}_i\tilde{D}_j W + \tilde{\gamma}_{ij}\left(\frac{1}{W}\tilde{D}_k\tilde{D}^k W - \frac{2}{W^2}\tilde{D}_k W \tilde{D}^k W\right).$$

```
auto W2Ricci_conf = evaluate(sym2_cast(
     1./2. * DDW  - 1./4.*W_sq_inv* tensor_cat(dW,dW)
   +1./2.*(divDW - 3/2.*contract(dW,dW_u)*W_sq_inv)*gammat));
```

```
if constexpr (std::is_same_v<simd<T, Abi>,
              simd<double, Vc::simd_abi::__avx512>>) {
   return static_cast<simd<double, Vc::simd_abi::__avx512>>(
   _mm512_castsi512_pd(_mm512_alignr_epi64(
   _mm512_castpd_si512(static_cast<__m512d>(b)),
   _mm512_castpd_si512(static_cast<__m512d>(a)), Shift)));
}
```

(M. Kretz, Vc Library,
ISO C++ Parallelism TS2)
https://github.com/VcDevel/Vc

GRMHD and Force-Free

- Complete CFD module has 100% vector register use
- Limited interpolation(WENO5) has same cost in all direction, also for non-contiguous directions. (About 6% of total runtime)
- Made sure all memory access is vectorized and aligned with cache line.
- Non-linear root-finding fully vectorized using masked assignment

```
if (abs(R) < 1. && nn > 2) {
   press_pp = press_prev;
   press_prev = press;
   press = Paitken;
   an += (press - press_prev) *
          rhostari;
 };
```

```
auto mask = (abs(R) < 1.) && (!mask_conv);
if (any_of(mask) && nn > 2) {
  where(mask, press_pp  )= press_prev;
  where(mask, press_prev)= press;
  where(mask, press     )= Paitken;
  where(mask, an        )+= (press - press_prev) * rhostari;
};
```

Efficient use of the HPC architecture

Skylake-X workstation

Elapsed Time: 105.481s

SP GFLOPS: 177.005

On average: 20.5% peak performance

Effective Physical Core Utilization: 97.5% (7.803 out of 8)

Effective Logical Core Utilization: 94.6% (15.135 out of 16)

EffectiveCPU Utilization Histogram

Memory Bound: 42.8% of Pipeline Slots

Memory limited: 42.8%!!

Cache Bound	15.2%	of Clockticks
DRAM Bound	36.7%	of Clockticks
DRAM Bandwidth Bound	31.3%	of Elapsed Time
NUMA: % of Remote Accesses	0.0%	

Bandwidth Utilization Histogram

Explore bandwidth utilization over time using the histogram and identify memory objects or functions with maximum contribution to the high bandwidth utilization.

Bandwidth Domain: DRAM, GB/sec

Bandwidth Utilization Histogram

This histogram displays the wall time the bandwidth was utilized by certain value. Use sliders at the bottom of the histogram to define thresholds for Low, Medium and High utilization levels. You can use these bandwidth utilization types in the Bottom-up view to group data and see all functions executed during a particular utilization type. To learn bandwidth capabilities, refer to your system specifications or run appropriate benchmarks to measure them; for example, Intel Memory Latency Checker can provide maximum achievable DRAM and interconnect bandwidth.

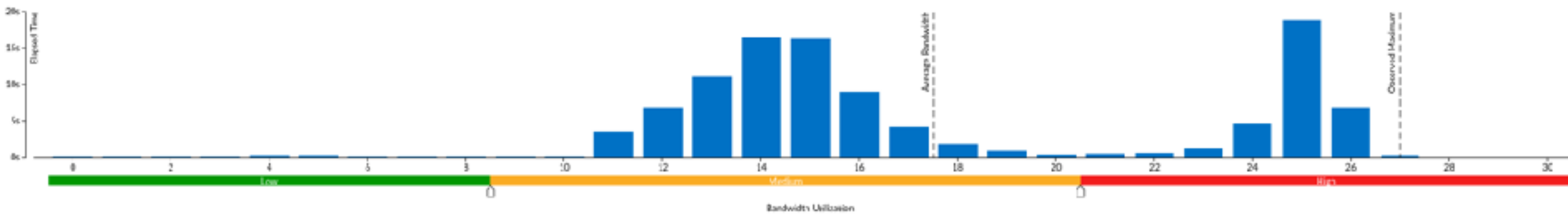

Top Functions with High Bandwidth Utilization

This section shows top functions, sorted by LLC Misses that were executing when bandwidth utilization was high for the domain selected in the histogram area.

Function	LLC Miss Count
[Loop at line 1843 in amrex::BaseFab<double>::copy]	8.7%
[Loop at line 271 in amrex::MultiFab::Saxpy_omp_fn.7]	6.0%
[Loop at line 582 in amrex::FabArray<amrex::FArrayBox>::ParallelCopy._omp_fn.9]	5.3%
[Loop at line 242 in amrex::MultiFab::LinComb._omp_fn.9]	4.4%
[Loop at line 1704 in amrex::FabArray<amrex::FArrayBox>::mult<std::enable_if<(bool)1, void>>._omp_fn.27]	3.5%
[Others]	1.5%

N/A is applied to non-summable metrics.

Memory access dominated by AMReX routines!

FPU Utilization: 5.1%

SP FLOPs per Cycle	3.252 Out of 64
Vector Capacity Usage	99.1%
FP Instruction Mix:	
% of Packed FP Instr.	99.9%
% of 128-bit	0.0%
% of 256-bit	1.5%
% of 512-bit	98.4%
% of Scalar FP Instr.	0.1%

AVX512: 99.1% vectorization!

Efficient use of large machines

FRONTERA

Weak scaling

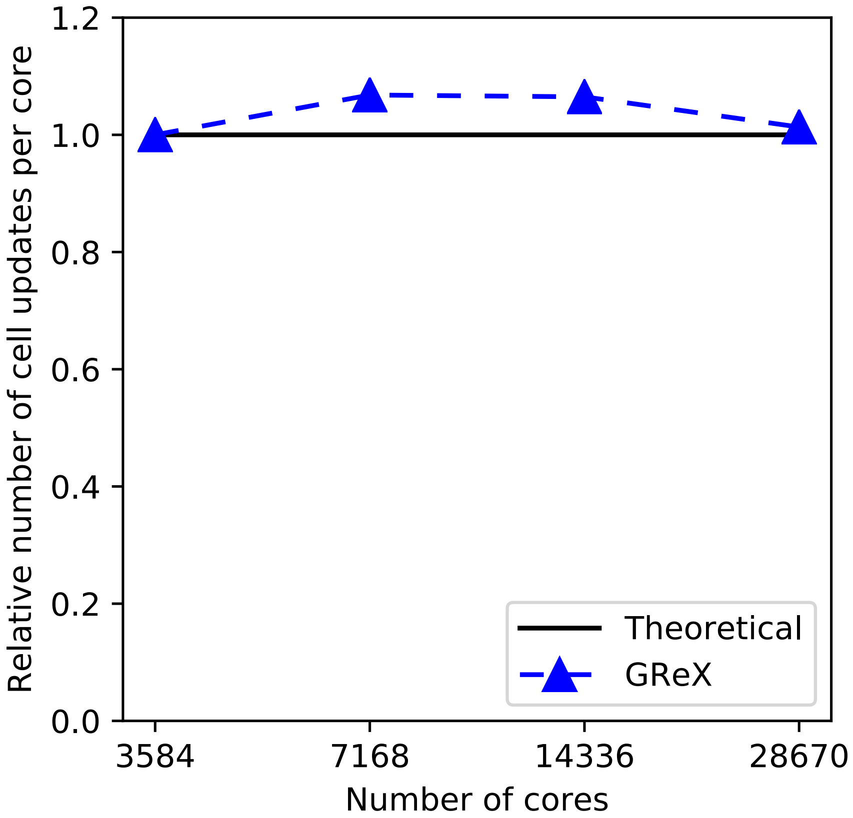

Strong scaling

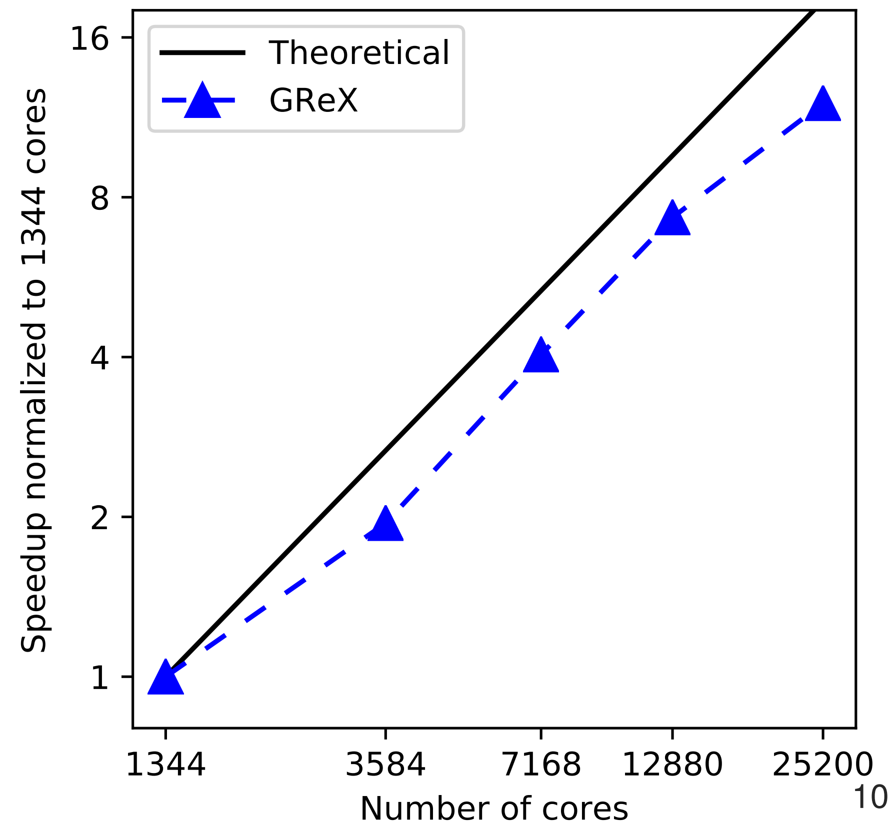

SuperMUC-NG

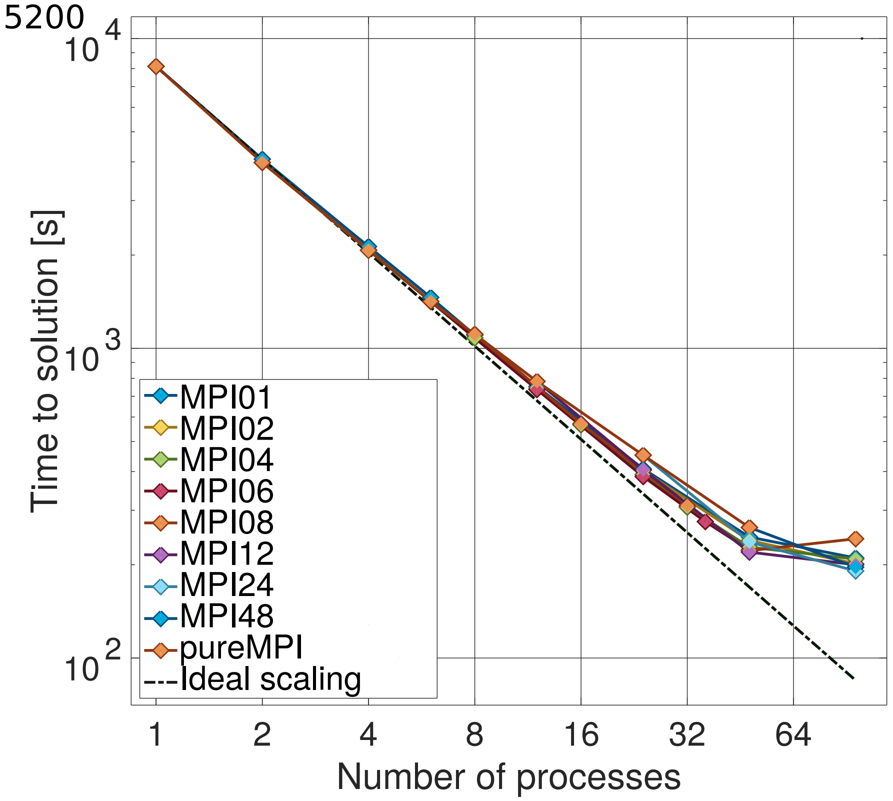

- Excellent single and multi-node scaling.
- Code has been optimized on SuperMUC-NG with help of HPC-tuning staff (AstroLab)

Electromagnetic precursors

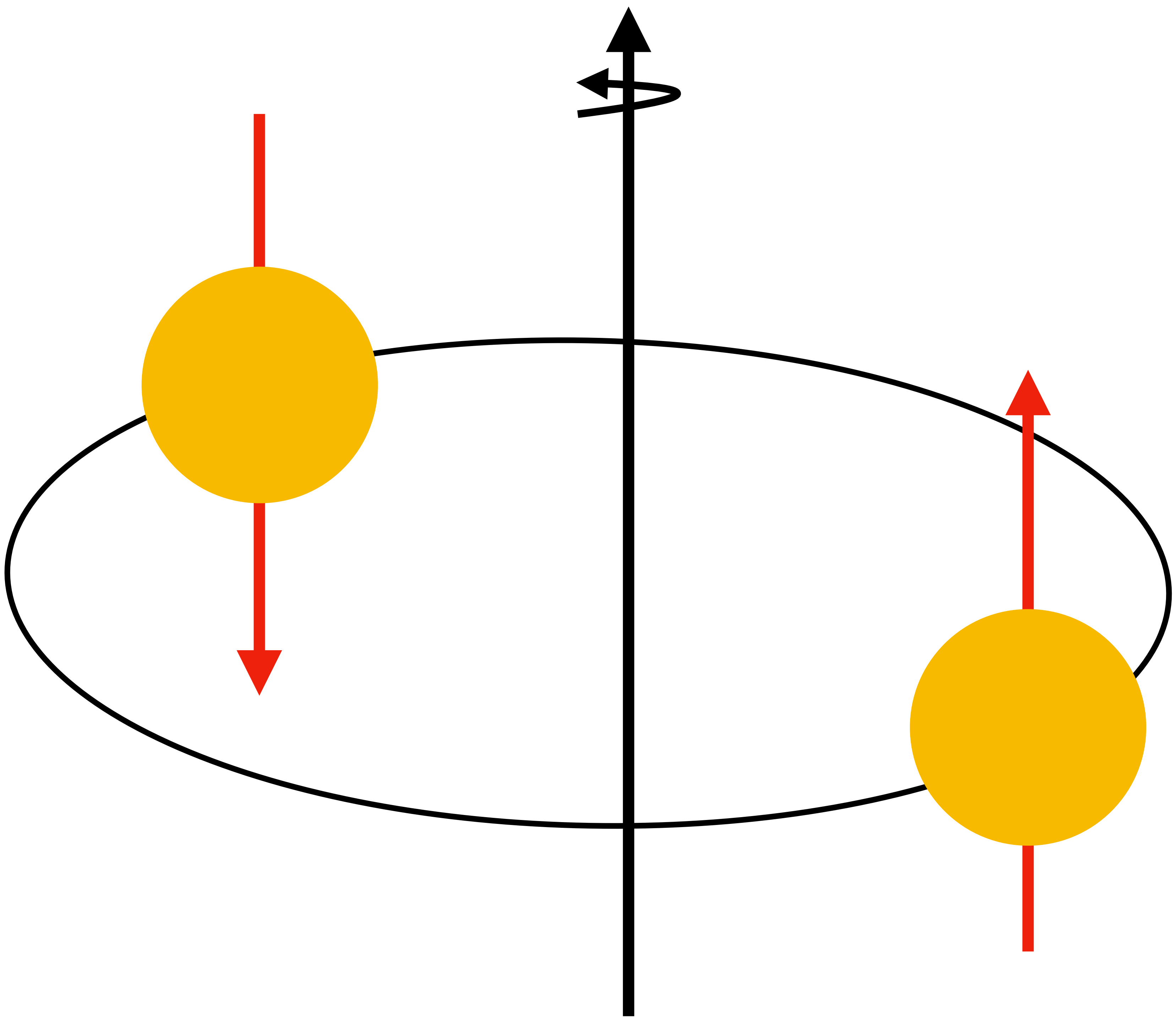

Electromagnetic precursors

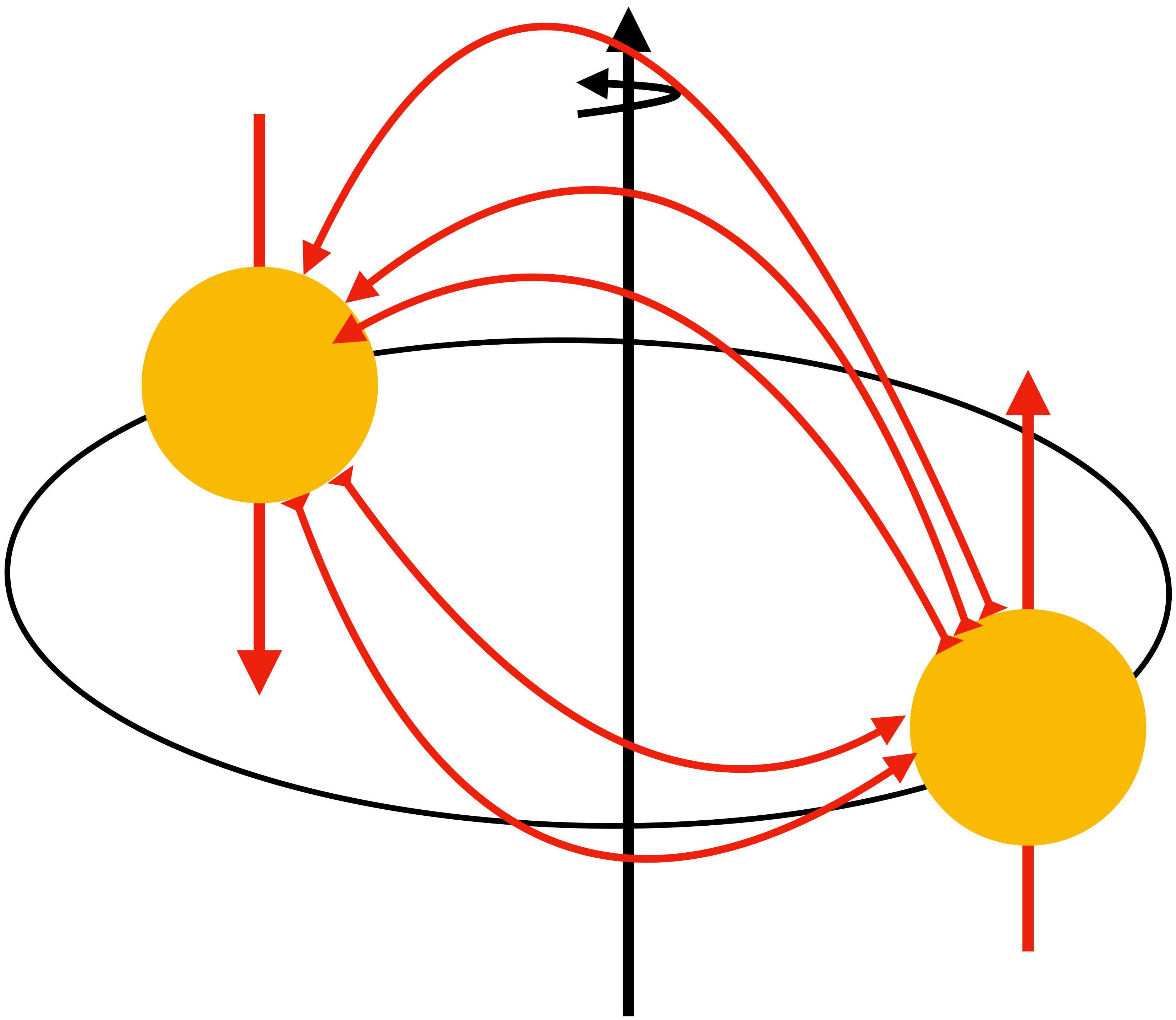

Electromagnetic precursors

Adding the right twist

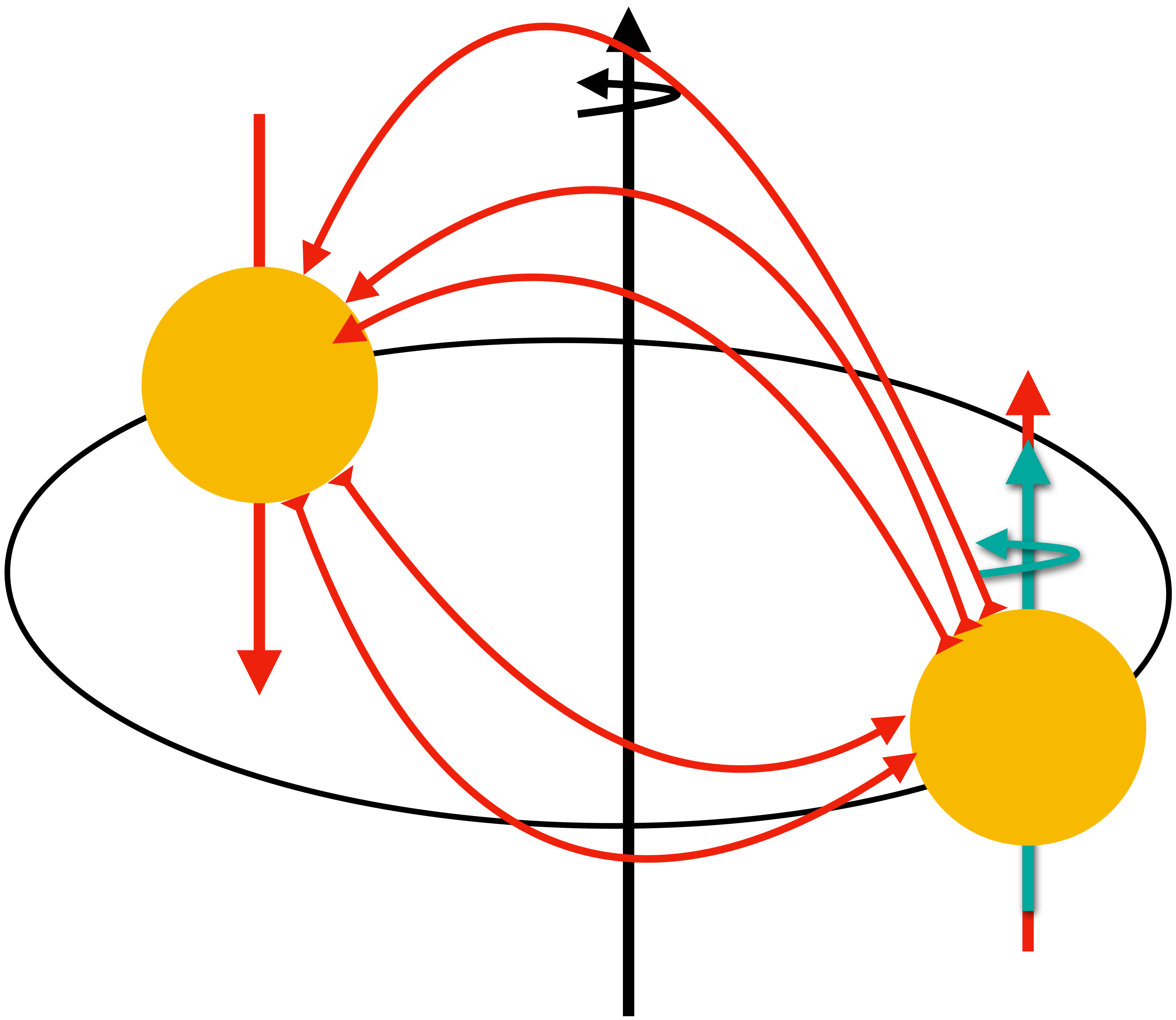

Electromagnetic precursors
Adding the right twist

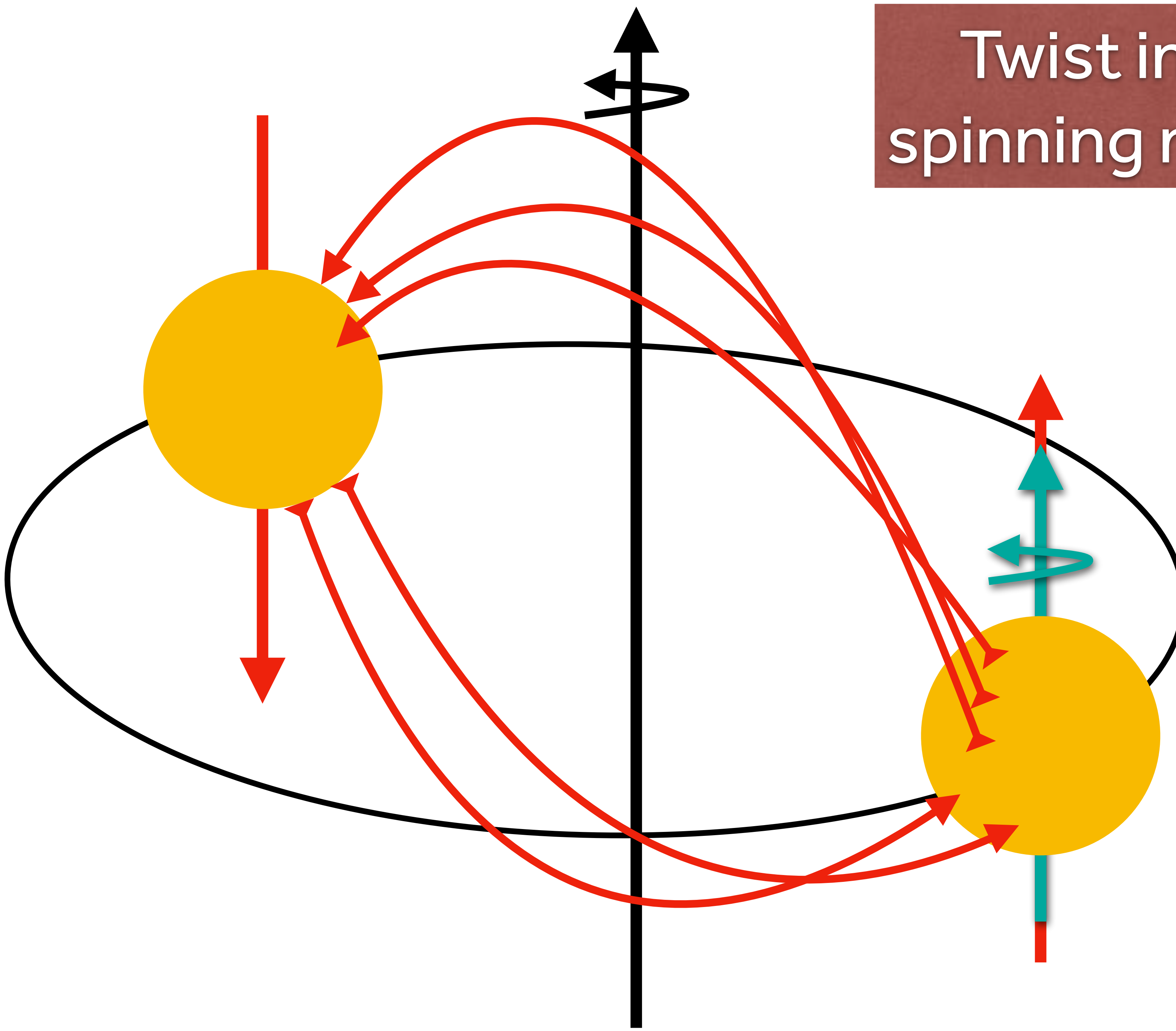

Twist induced by spinning neutron star

Electromagnetic precursors

3D Force-free electrodynamics simulation

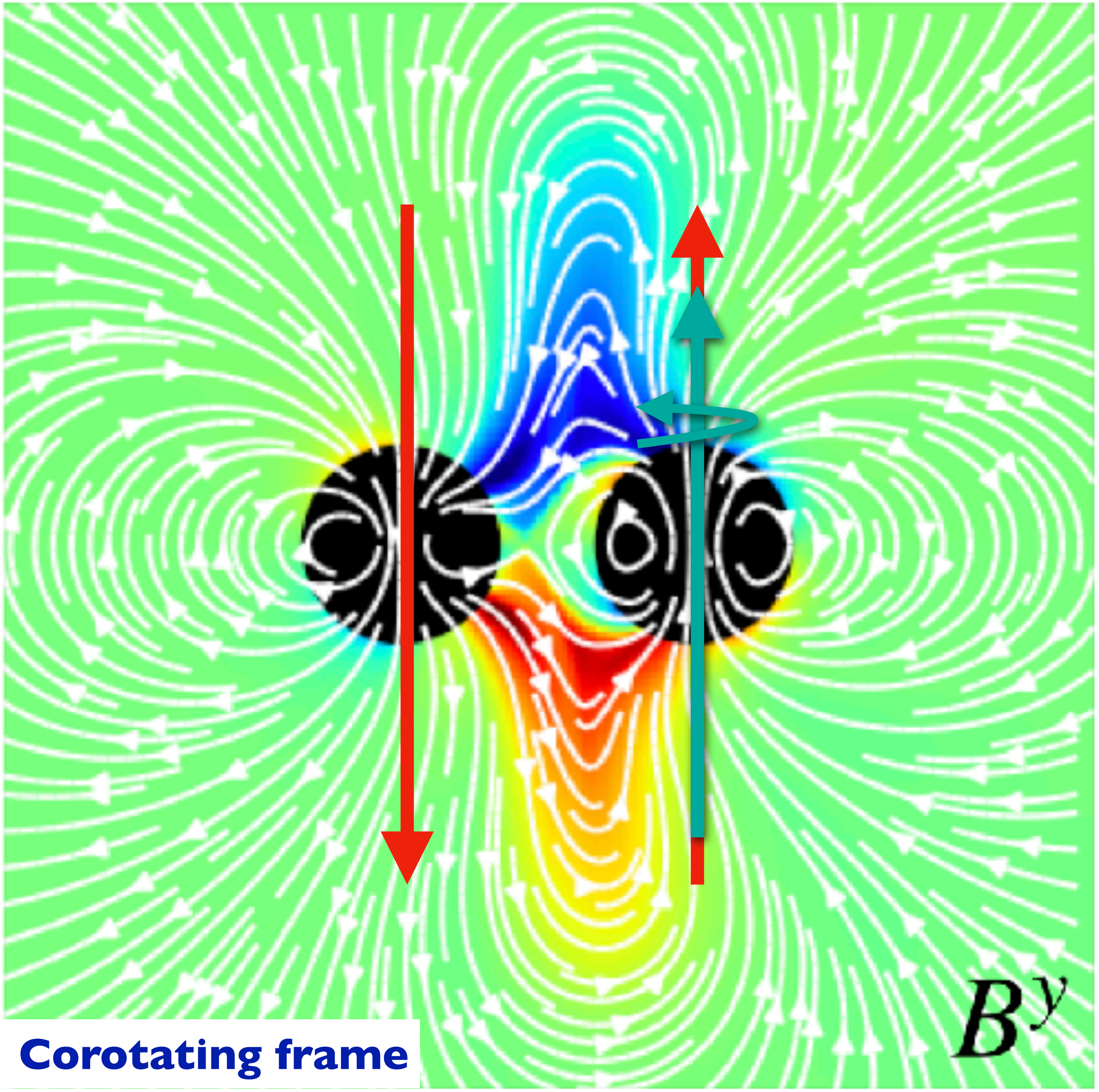

ERM & Philippov
(ApJL 2020)

Pre-merger flaring

3D Force-free electrodynamics simulation

time (orbits) = 0.42

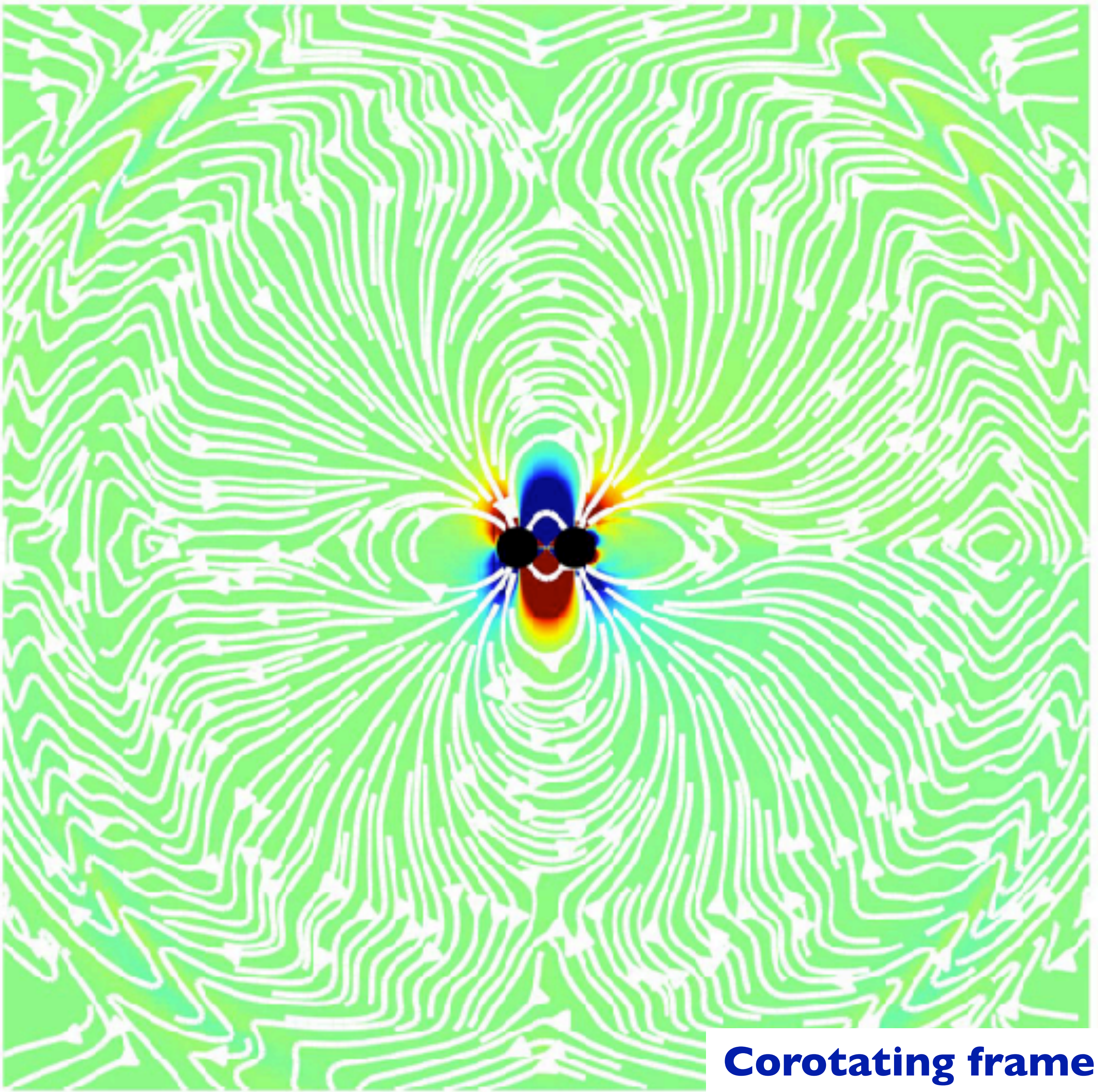

Corotating frame

ERM & Philippov (ApJL 2020)

Emission mechanism

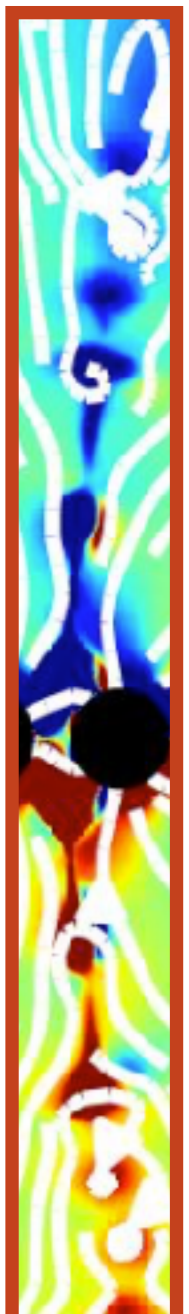

- Need to convert the emitted electromagnetic energy into coherent radio waves!
- Electromagnetic fireball similar to the one in magnetar model of FRBs (maser emission from magnetized shock) Lyubarsky (2014), Beloborodov (2017)

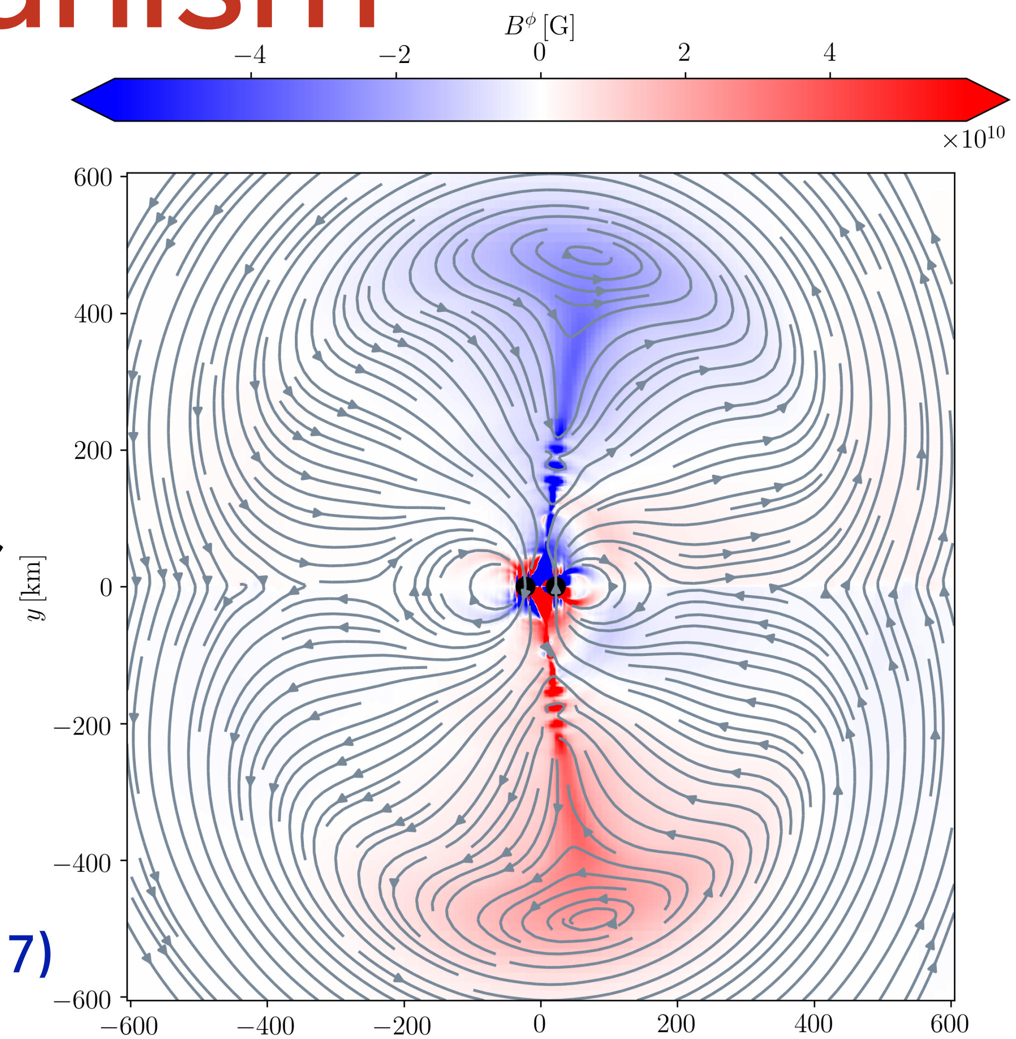

- Merger of plasmoids promise to be another potential channel for coherent radio emission Philippov+(2019)

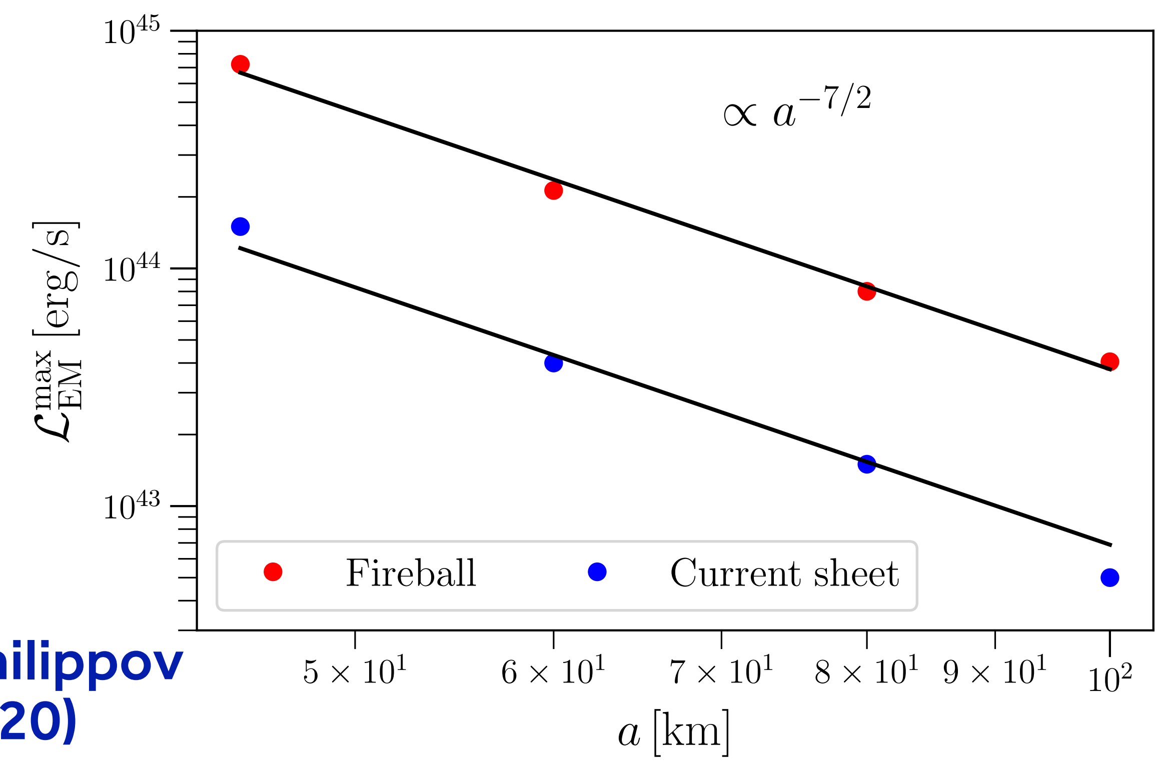

ERM & Philippov (ApJL 2020)

How much energy can we dissipate?

- Emission of flares is periodic with orbital parameters.
- This dissipative power and emission will depend on the fraction of field lines that can be twisted (and which eventually reconnect).

$$\mathcal{L}_{\rm EM}^{\rm max} = \frac{\Delta E_{\rm twist}}{\Delta t} \approx \eta \frac{\psi^2}{2} v_{\rm rec} \frac{R^3}{a^4} E_0$$

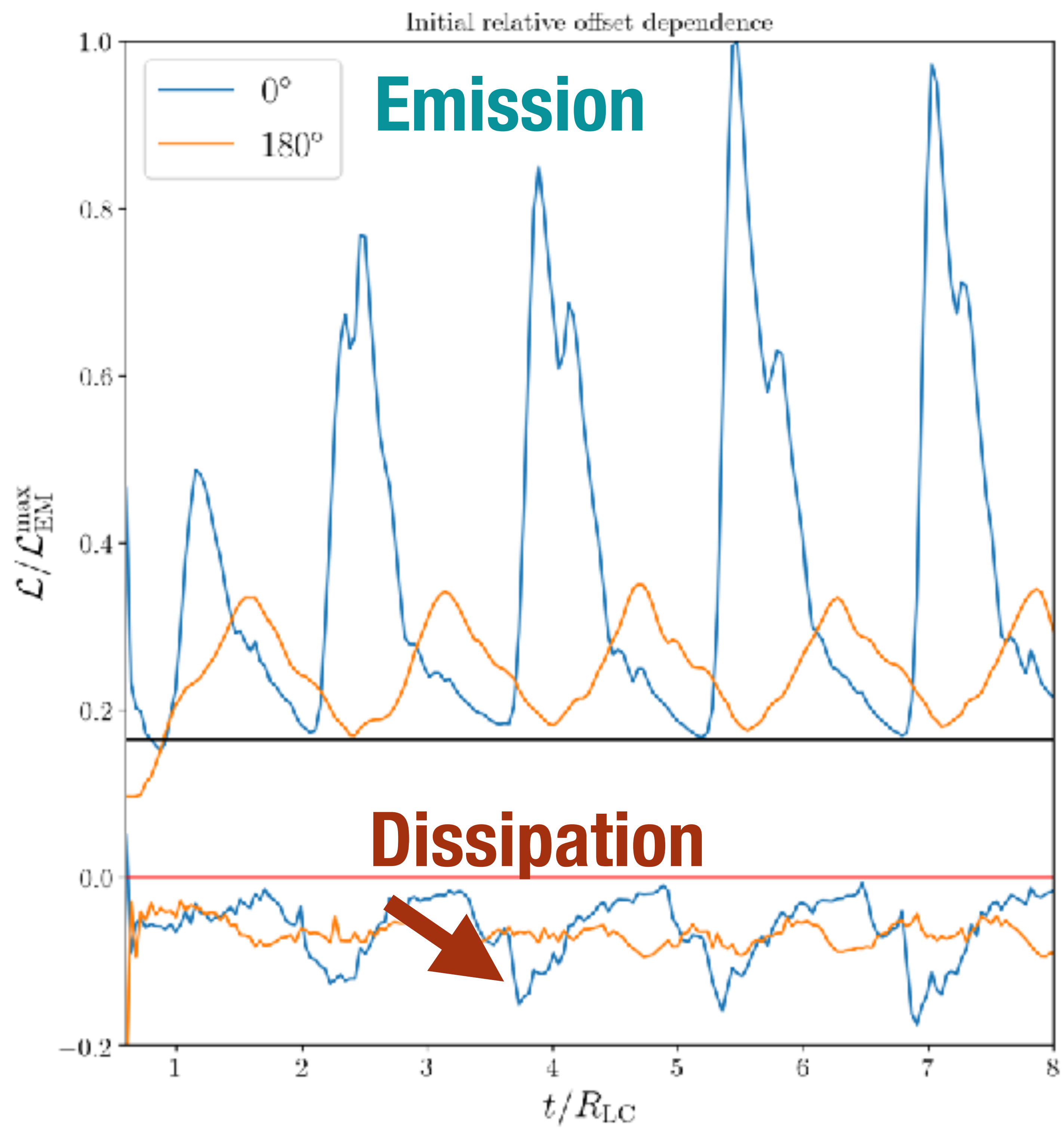

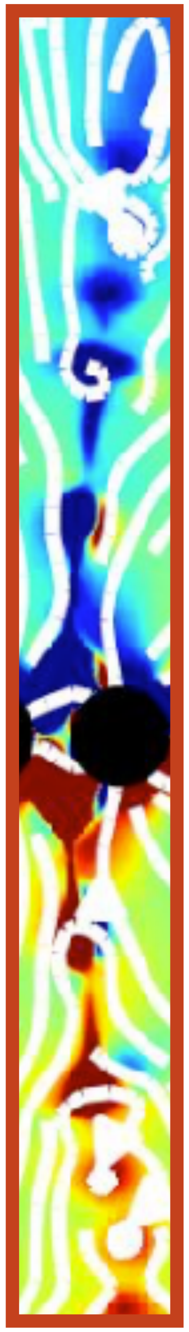

Exploring the parameter space

Flaring happens for different alignments and magnetizations

different tilts

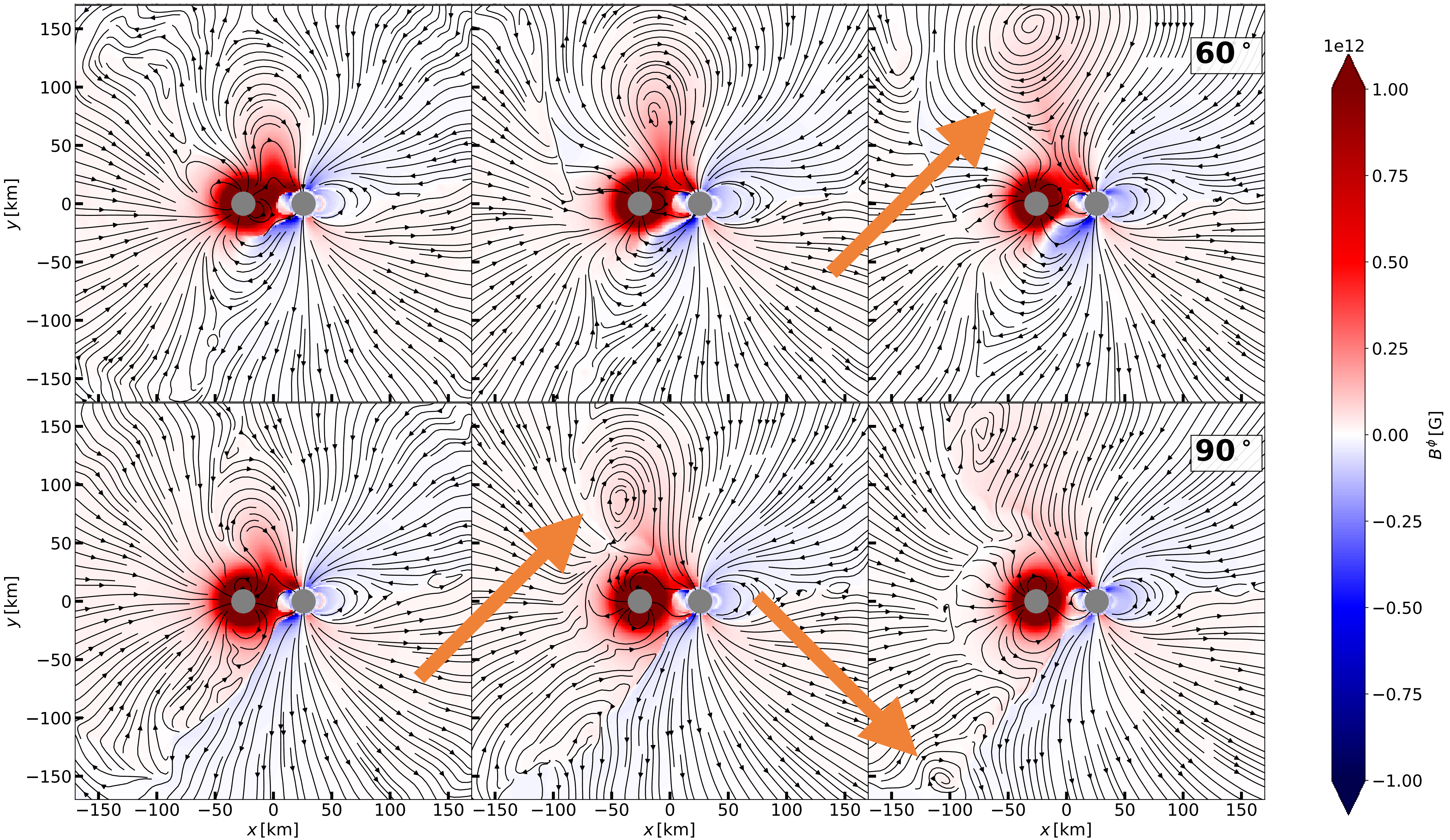

ERM & Philippov
(in prep)

Exploring the parameter space

Flaring happens for different alignments and magnetizations

10x weaker field

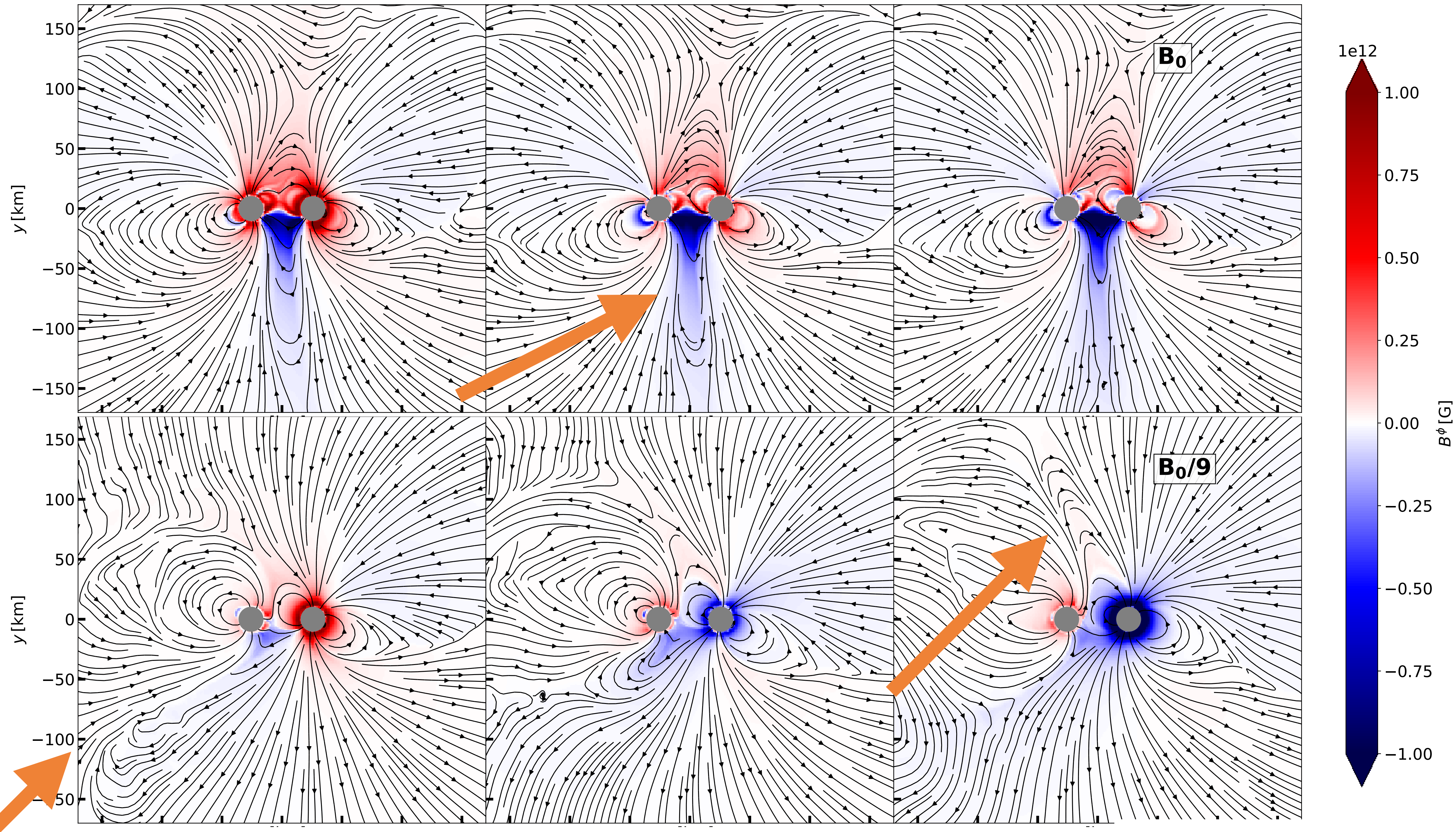

ERM & Philippov
(in prep)

Exploring the parameter space

- X-ray timing of the NICER mission has revealed that PSR J0030+0451 has a multipolar field structure. **Bilous+(2019)**

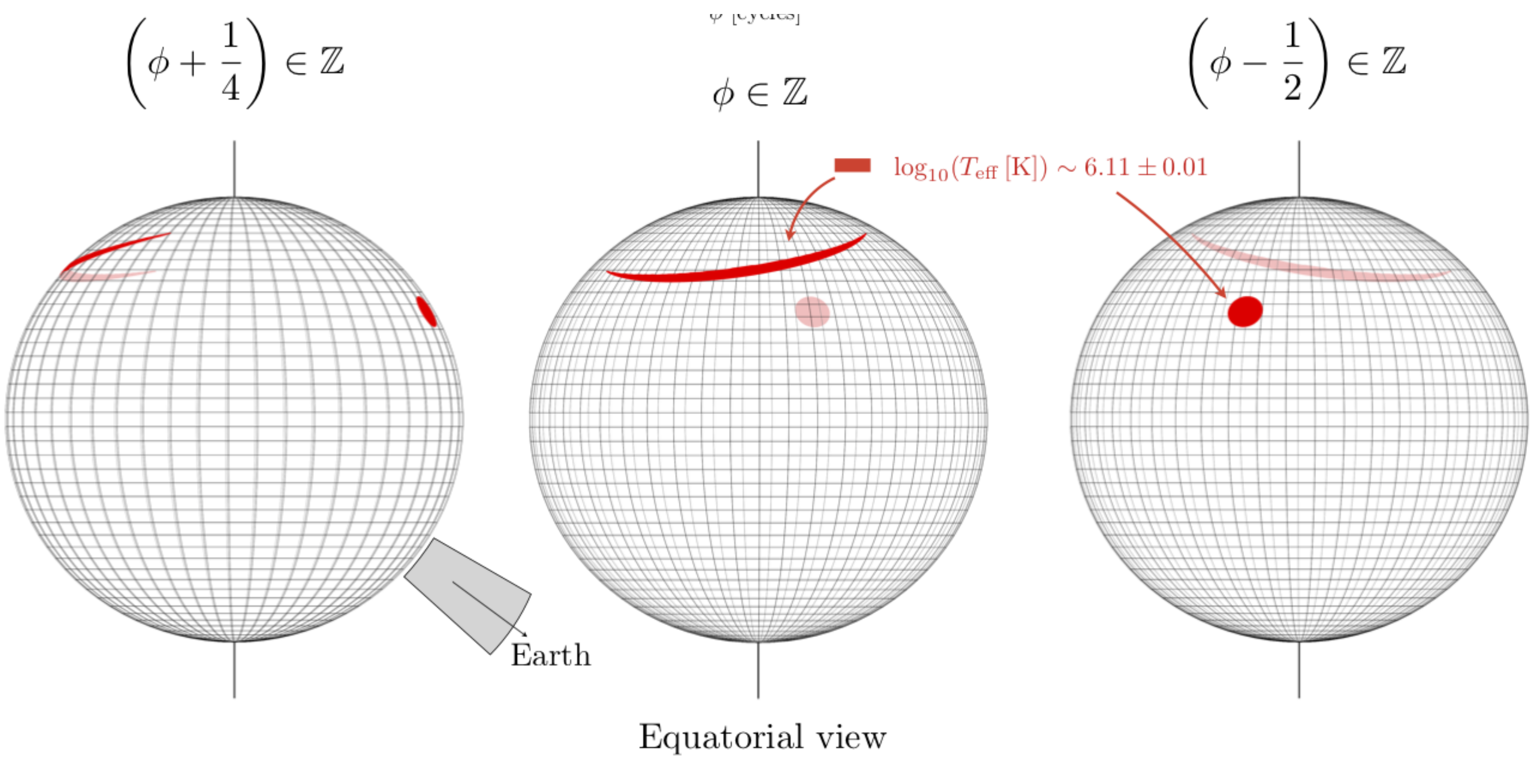

Riley+(2019)

Exploring the parameter space

- X-ray timing of the NICER mission has revealed that PSR J0030+0451 has a multipolar field structure. **Bilous+(2019)**

Does flaring still work in this case?

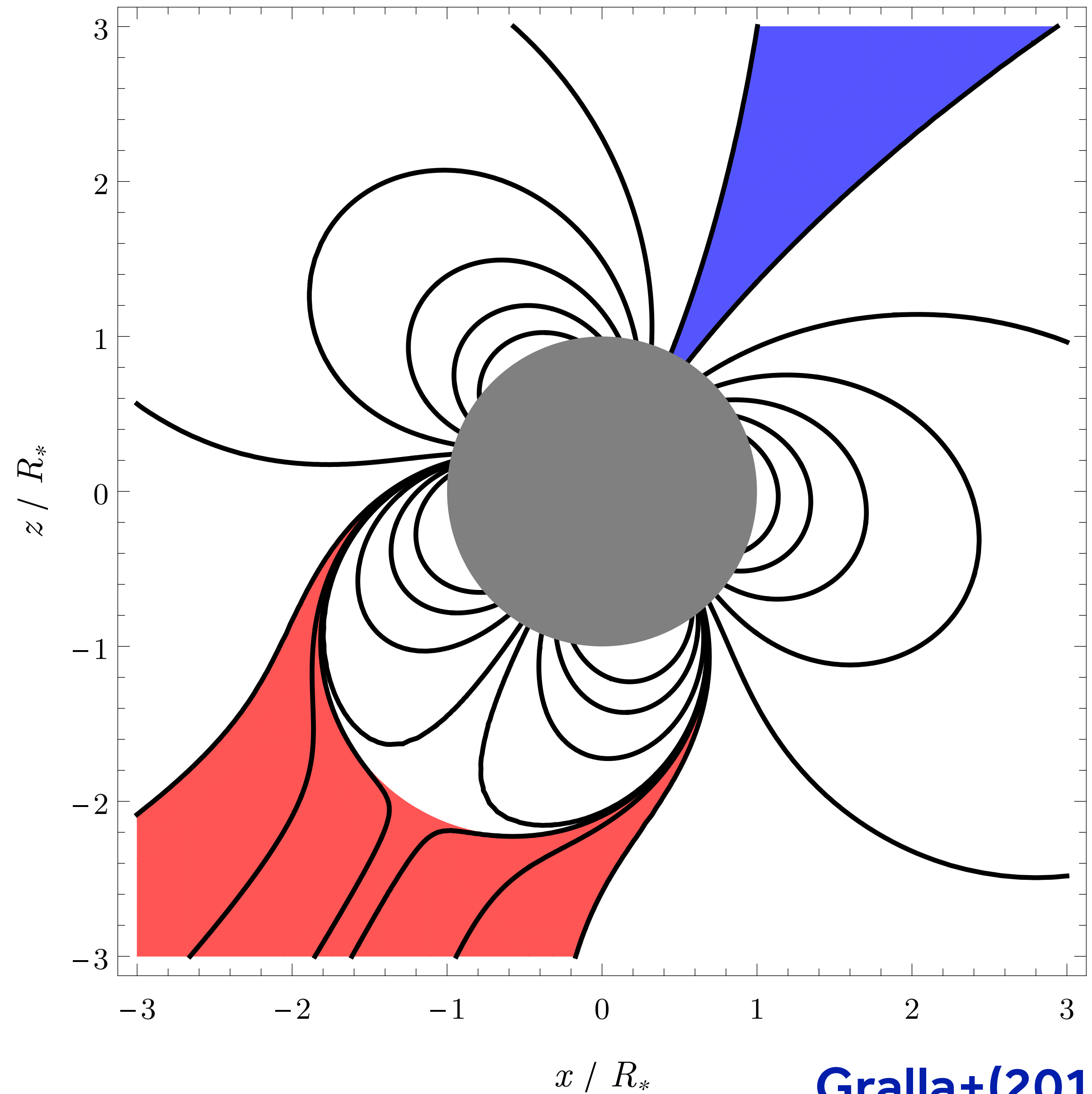

Gralla+(2017)

Exploring the parameter space

Flaring happens for different topologies

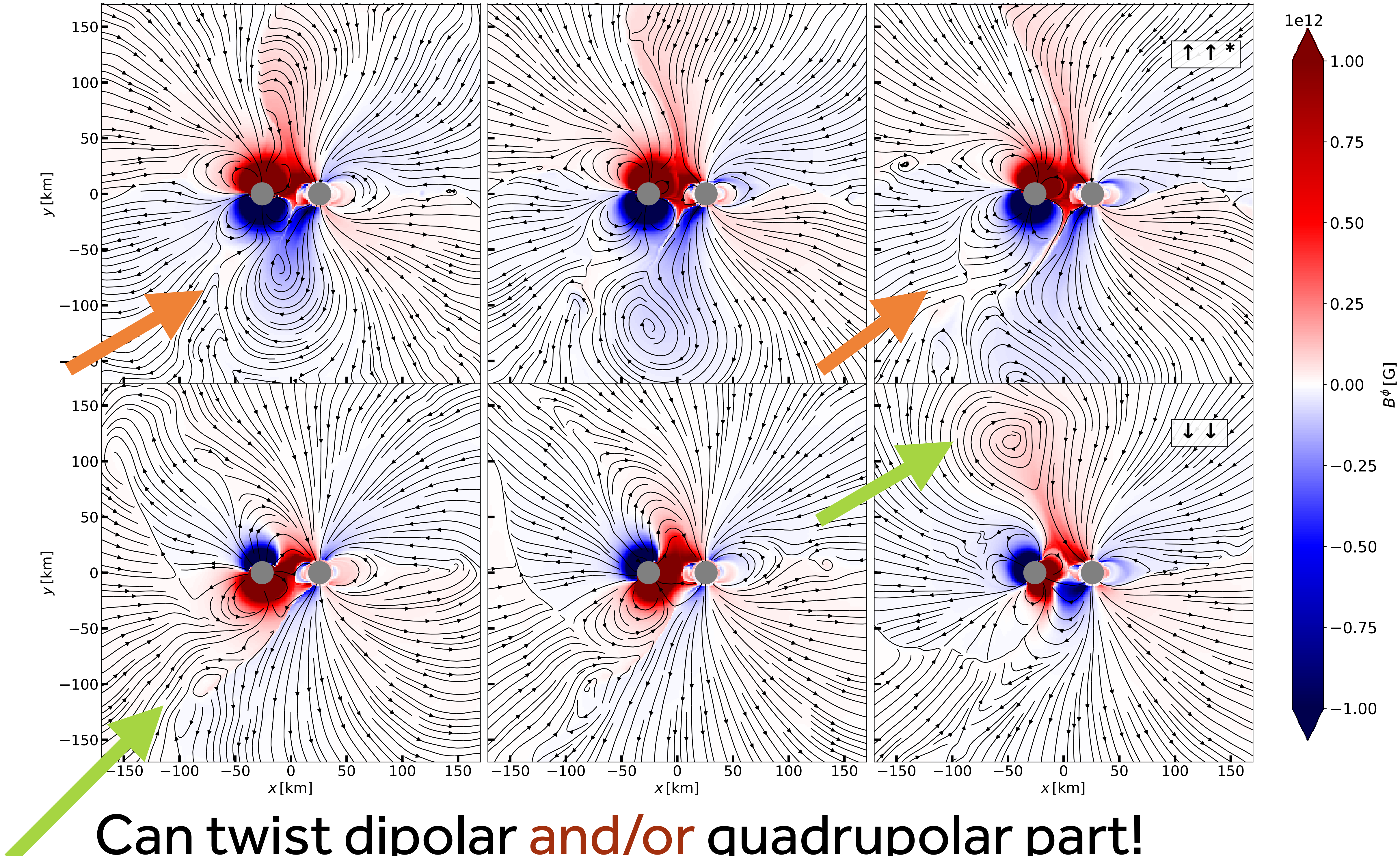

Can twist dipolar and/or quadrupolar part!

ERM & Philippov (in prep)

Outlook: Flares in magnetars

Flares can also be launched from twisted magnetar magnetospheres

Parfrey+(2012)

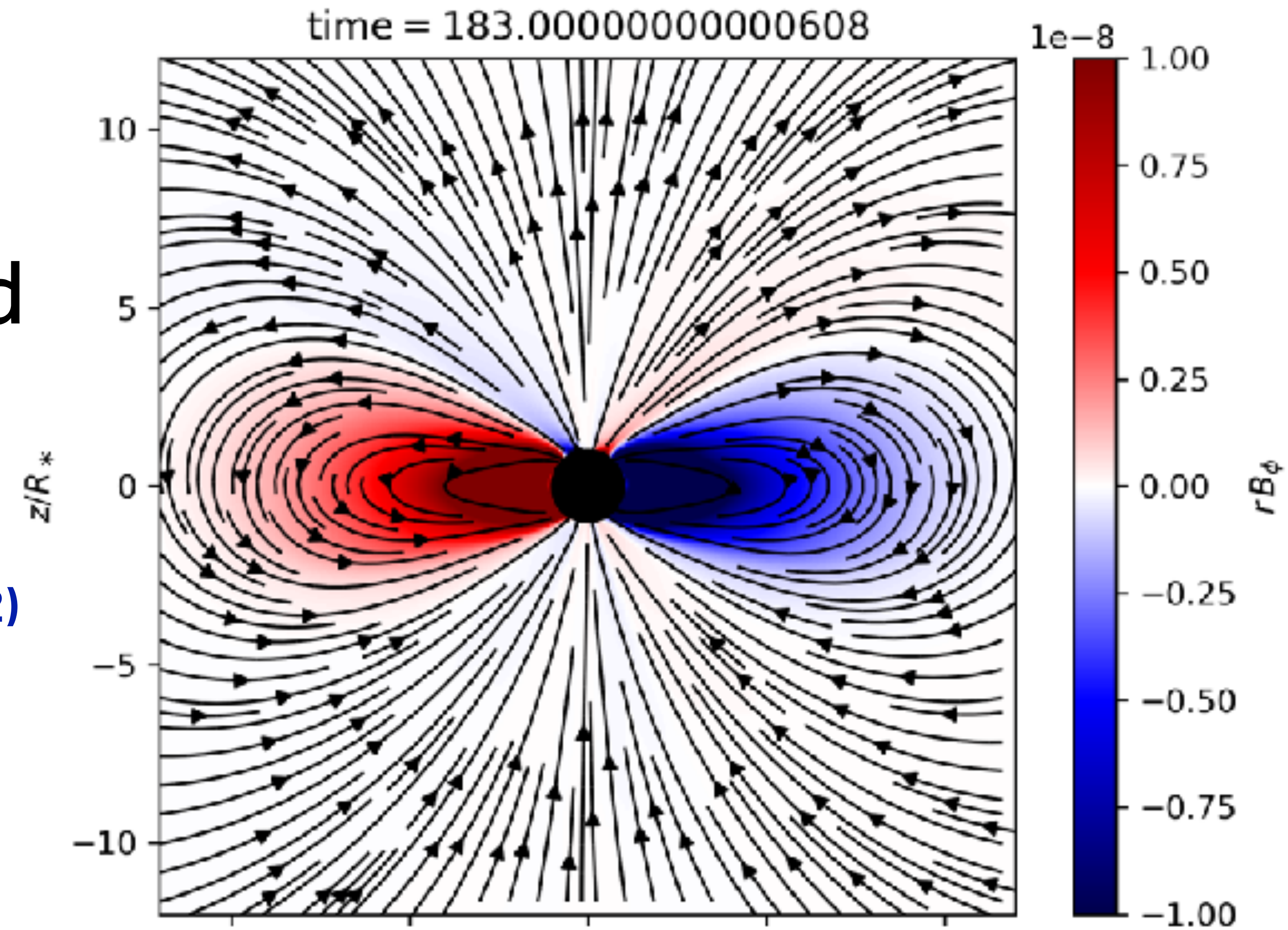

Highly relevant in the context of recent Fast Radio Burst observations from galactic magnetars

Bochenek+(2020)

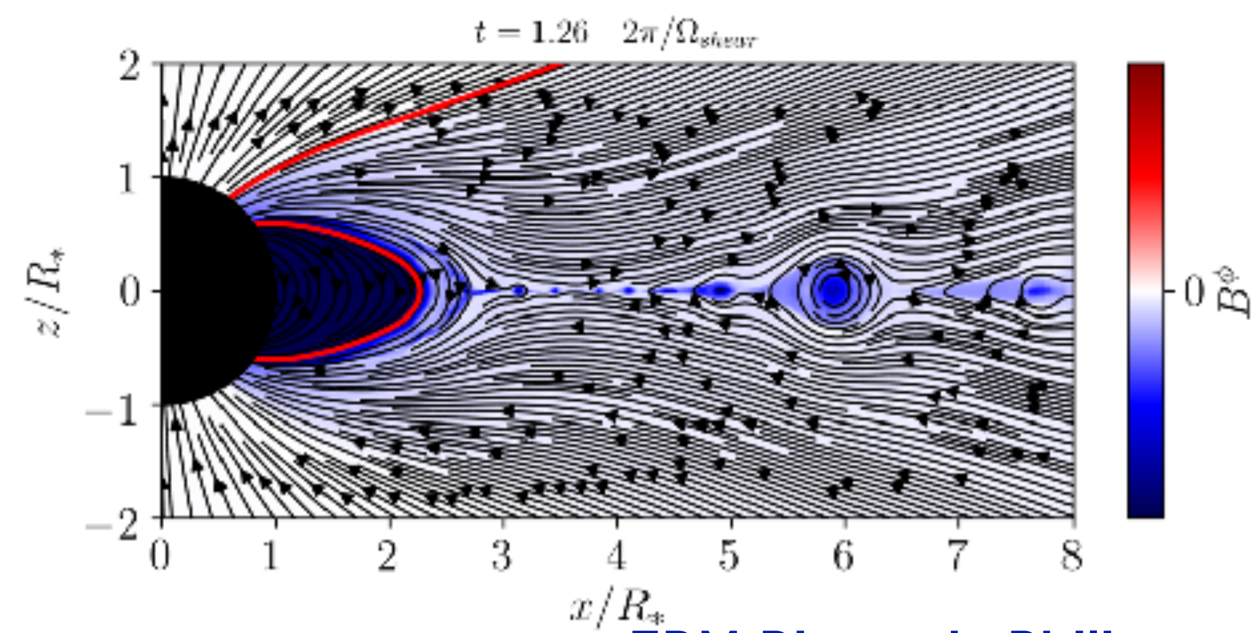

ERM,Ripperda,Philippov+(in prep)

Outlook: Alfen waves in magnetars

Instead of magnetar giant flares, it is also possible to consider non-linear Alfven wave interactions. Yuan+(2020)

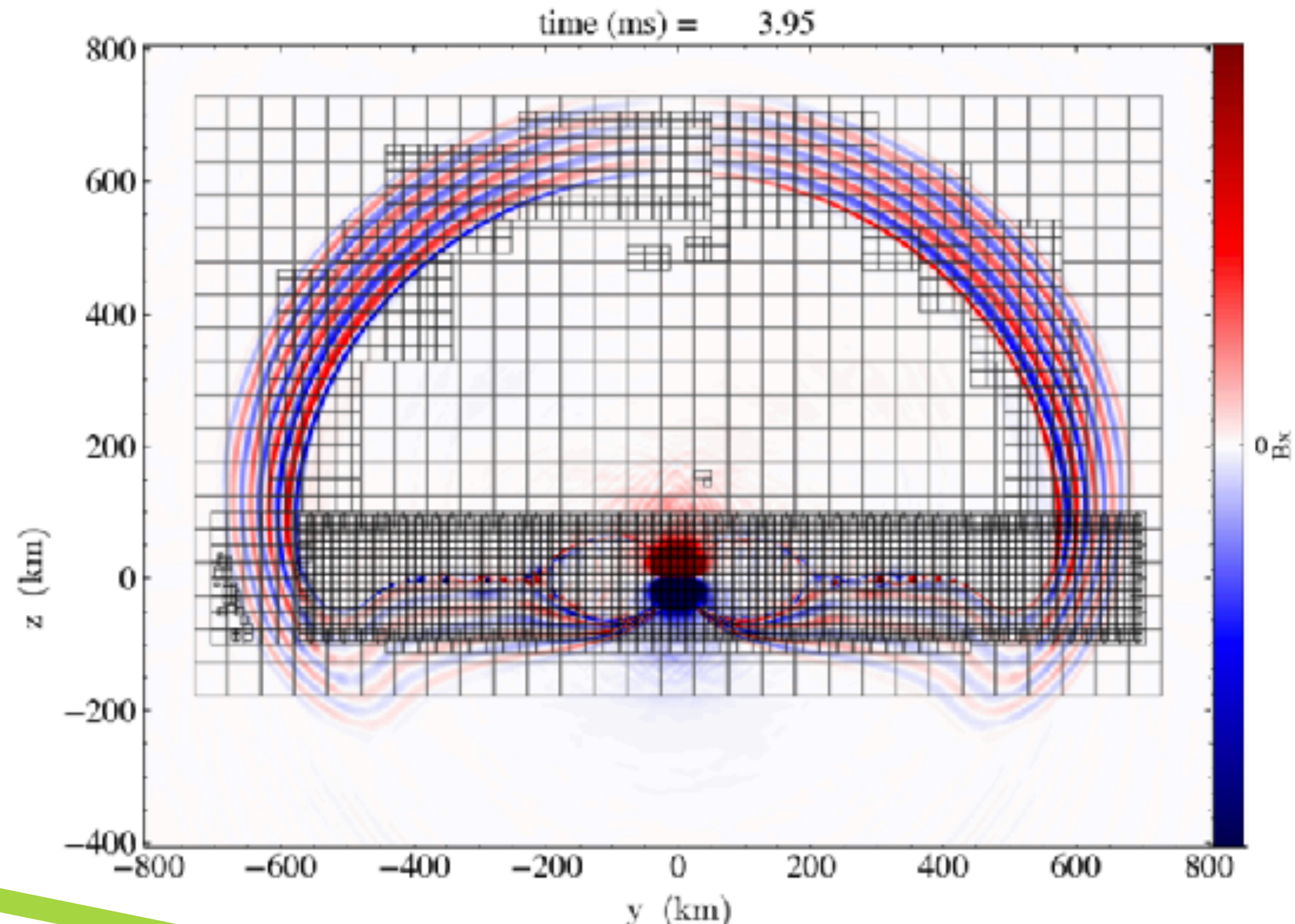

Since the plasmoid formation in the current sheet happens at large scales, can leverage **adaptive mesh refinement.**

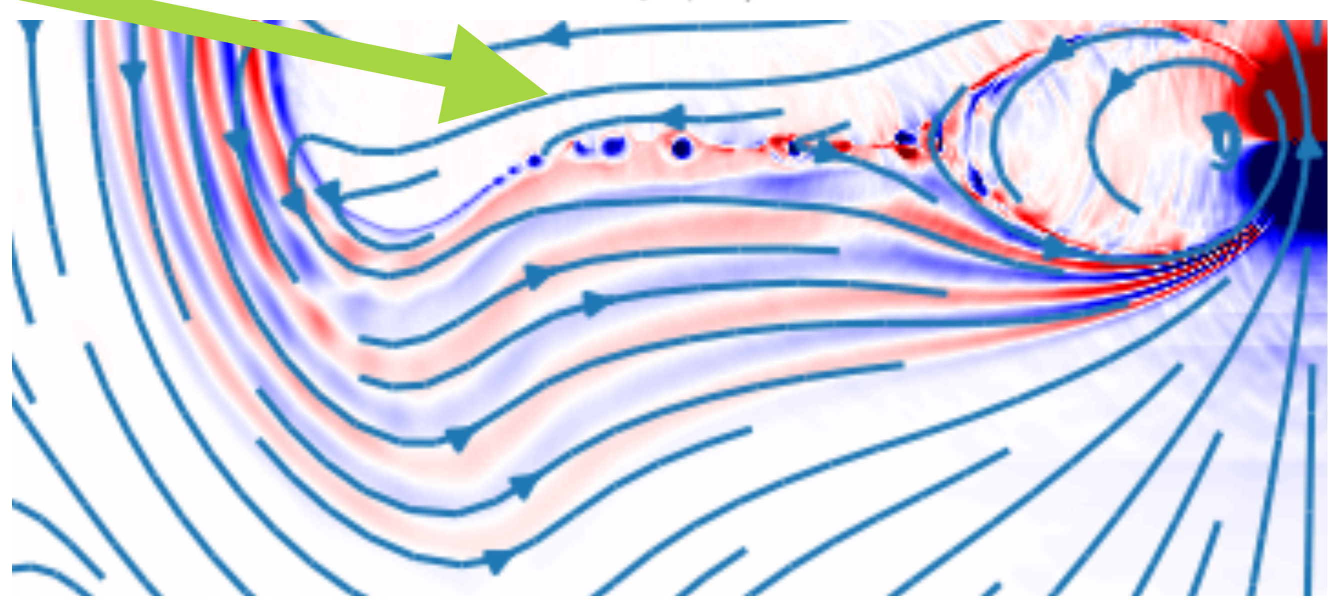

ERM,Philippov+(in prep)

Outlook: Balding black holes

A very similar phenomenon happens for balding black holes.

Lyutikov+(2011)

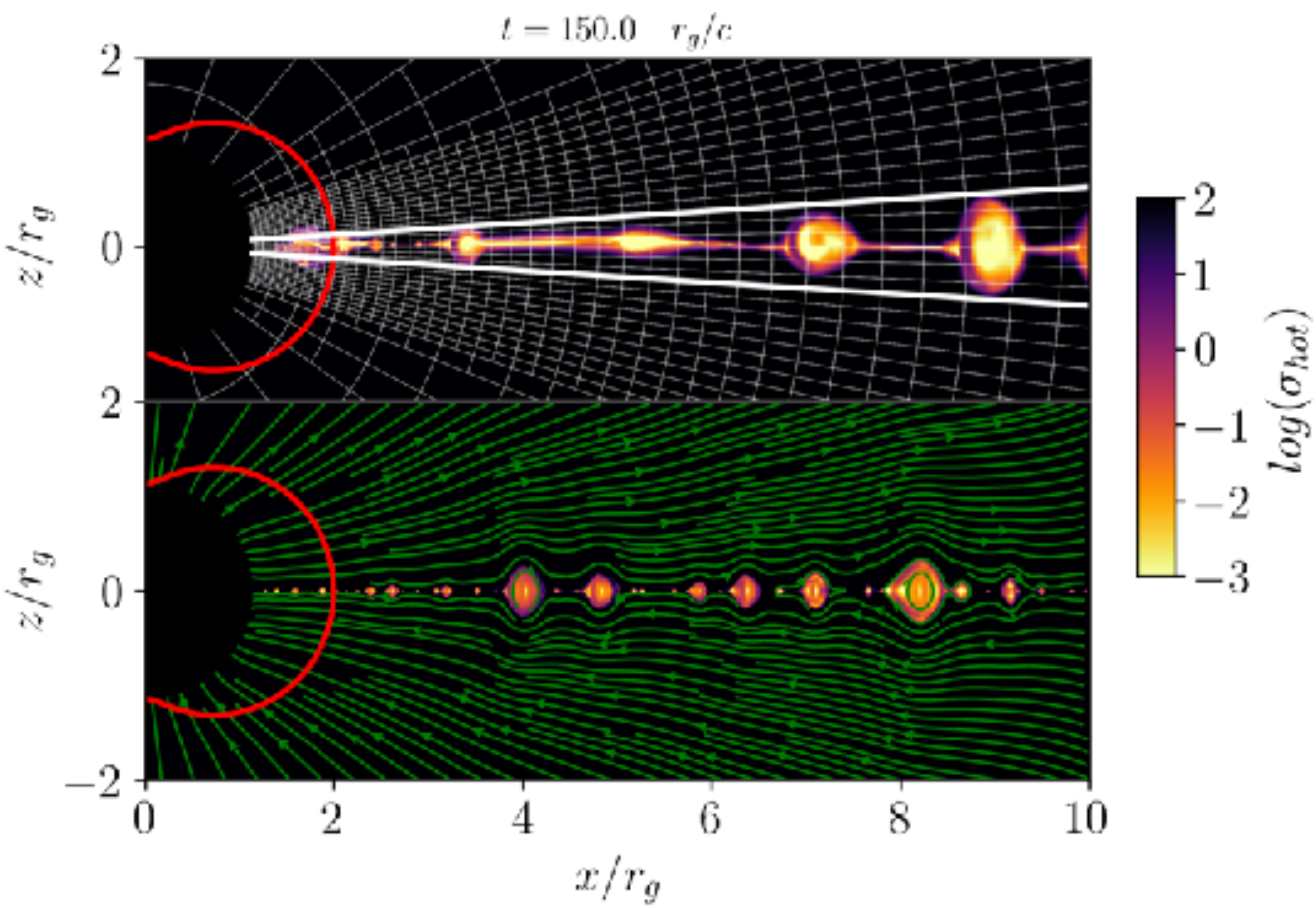

Bransgrove, Ripperda & Philippov(in prep)

Transitioning from an initial dipolar field (e.g. from collapsing neutron star) to a split monopole solution causes the field lines to reconnect.

Conclusions

Twisting of magnetic field lines before the merger can launch powerful electromagnetic flares for a wide range of orbital parameters